

Review

Polysaccharides-Based Injectable Hydrogels: Preparation, Characteristics, and Biomedical Applications

Naglaa Salem El-Sayed  and Samir Kamel * 

Cellulose and Paper Department, National Research Centre, Cairo 12622, Egypt

* Correspondence: samirki@yahoo.com

Abstract: Polysaccharides-based injectable hydrogels are a unique group of biodegradable and biocompatible materials that have shown great potential in the different biomedical fields. The biomolecules or cells can be simply blended with the hydrogel precursors with a high loading capacity by homogenous mixing. The different physical and chemical crosslinking approaches for preparing polysaccharide-based injectable hydrogels are reviewed. Additionally, the review highlights the recent work using polysaccharides-based injectable hydrogels as stimuli-responsive delivery vehicles for the controlled release of different therapeutic agents and viscoelastic matrix for cell encapsulation. Moreover, the application of polysaccharides-based injectable hydrogel in regenerative medicine as tissue scaffold and wound healing dressing is covered.

Keywords: polysaccharides; injectable hydrogel; injectable mechanisms; biomedical applications



Citation: El-Sayed, N.S.; Kamel, S. Polysaccharides-Based Injectable Hydrogels: Preparation, Characteristics, and Biomedical Applications. *Colloids Interfaces* **2022**, *6*, 78. <https://doi.org/10.3390/colloids6040078>

Received: 31 August 2022

Accepted: 28 November 2022

Published: 8 December 2022

Publisher's Note: MDPI stays neutral with regard to jurisdictional claims in published maps and institutional affiliations.



Copyright: © 2022 by the authors. Licensee MDPI, Basel, Switzerland. This article is an open access article distributed under the terms and conditions of the Creative Commons Attribution (CC BY) license (<https://creativecommons.org/licenses/by/4.0/>).

1. Introduction

Polysaccharides (PSs) are abundant and reproducible natural polymers that consist of monosaccharide units linked together through glycosidic bonds. These polymers can have a linear or branched structure, with one type of monosaccharide building unit (homopolysaccharides), or contain two or more types of monosaccharide units (heteropolysaccharide) [1]. Natural PSs have various extraction resources, such as marine algae, weeds, plants, microbes, and animals (Figure 1). Meanwhile, semi-synthetic PSs such as chitosan and cellulose ethers are produced by the chemical or enzymatic modifications of the parent polysaccharides [2–4]. Moreover, PSs can be classified according to their charge into positively charged polysaccharides, e.g., chitosan, negatively charged PSs, e.g., alginate, heparin, hyaluronic acid, pectin carrageenan, and neutrally charged PSAs, e.g., dextran, cellulose, and starch. The variation in the PSAs chemical composition, degree of polymerization, average molecular weight, and the diversity of the reactive functional groups (hydroxyl, carboxyl, and amino) potentially impacted their chemical reactivity [5,6]. Additionally, their mechanical stability, physicochemical diversity, and broad-spectrum biological activities such as microbial, antioxidant, anticoagulant, and antitumor certified them as suitable candidates for biomedical applications [7–11].

Hydrogel is a crosslinked polymer with a three-dimensional, microporous network structure that can retain water, swell, and de-swell without dissolving [12–14]. The presence of one or more hydrophilic functional groups (OH, CO₂H, SO₃H, or NH₂) along the hydrogel network grants the hydrogel the ability to absorb water. Moreover, the swelling rate of the hydrogel depends on the degree of crosslinking, and the external environments, such as pH, temperature, salts type, and concentration, mainly depend on the external environment [15,16]. Different techniques have been proposed for synthesizing and crosslinking the hydrogels, which could proceed parallel to polymerization or after growing the polymer chains. The degree of the polymer crosslinking controls these parameters in the hydrogel, such as the elastic modulus, swelling properties, surface morphology, and network porosity [17,18].

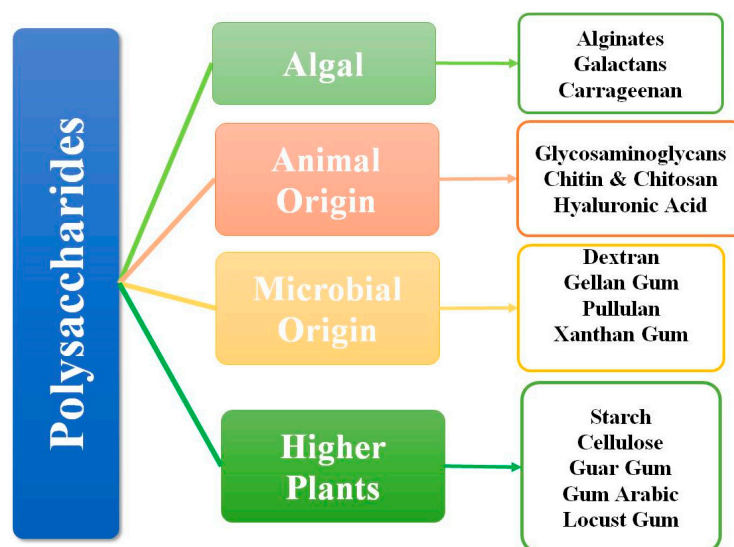


Figure 1. Natural polysaccharides: structural features and properties.

Polysaccharides-based injectable hydrogels (PSIHs) are a class of hydrogels that undergo sol-gel phase transition upon injection in response to physical, chemical, or biological stimuli [19]. The external stimuli could be changes in ionic strength, temperature, or visible light UV exposure. Like other conventional hydrogels, they are characterized by their ability to absorb and retain water, flexibility, porosity, 3D-dimensional structure, hydrophilic or amphiphilic nature, and softness. Moreover, their injectability, biocompatibility, and bio-degradability grant the hydrogels the credential to be employed extensively in various biomedical applications [20]. After loading the hydrogel precursors with the biologically active agent (e.g., drugs, proteins, enzymes, cells, vitamins, and natural extracts), they can be injected into living organisms through a tiny surgical hole using a syringe (Figure 2) [21]. In this review article, we intend to present the different methods used to fabricate injectable hydrogels based on polysaccharides and their applications in the encapsulation and release of therapeutics and regenerative medicine.

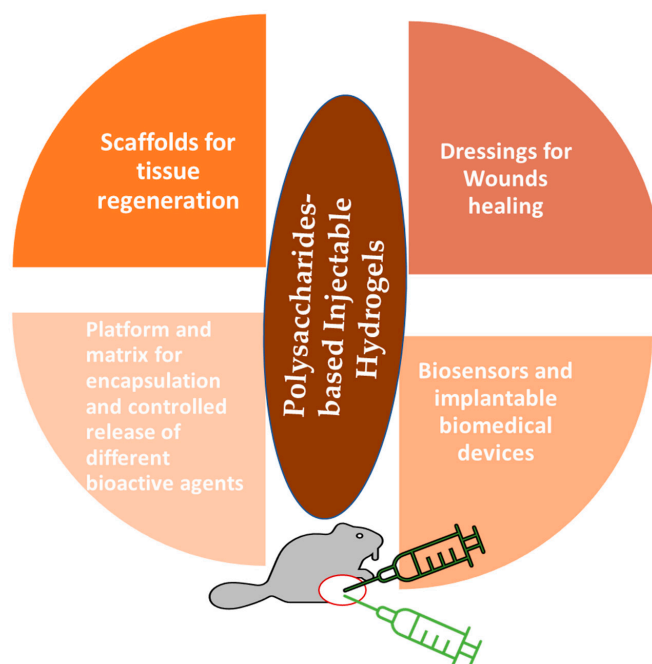


Figure 2. Different applications of polysaccharide-based injectable hydrogels (PSIHs).

2. Factors That Determine the Injectability of Hydrogels

The hydrogel is considered injectable if it can undergo a reversible sol-gel phase transition following the injection into the site of action in response to exposure to one or more external stimuli (visible light, UV light, change in temperature or pH, enzyme concentration) at the site of injection. Additionally, gelation kinetics (rate of transition from solution phase to gel phase) is an essential parameter in determining the injectability of the hydrogel. The viscosity and the ratio or concentration of the polymeric precursors, in addition to the method of coupling or crosslinking, are factors that control the rate of phase transition (gelation) and the degree of injectability. If the rate of phase transition is very slow, it can result in leakage of the hydrogel precursors before coupling, and if the rate is very high, it can cause clogging of the injection needle and inadequate dispersion and distribution of drugs into the IHS. Moreover, the mechanical properties of hydrogels strongly influence their ability to mimic tissues in biomedical applications IHS, which are used as tissue scaffolds, should display robust mechanical strength and stiffness to tolerate the repetitive mechanical deformation *in vivo*. Another critical factor is the hydrogel porosity; highly interconnected and highly organized porous networks, which can be micro- or nanoscale, according to the applications, are preferred for the hydrogel.

3. Preparation Techniques and Mechanism

Various approaches to preparing polysaccharide-based injectable hydrogels (PSIHS) have been explored. Polysaccharides, with their biocompatibility, physiochemical structure diversity, and flexibility for chemical modifications with additional functional moieties or linkers, are considered perfect candidates for the fabrication of IHS and can easily trigger the gelation process under physiological pH, body temperature, or UV exposure. Generally, hydrogel crosslinking can occur via one or more mechanisms, either physically or chemically, when the hydrogel precursors are subjected to an external stimulus (heat, UV irradiation, or pH change) [22–25]. The rate of hydrogel injectability is controlled by the chemical structure and concentration of the polymeric chains, the mechanism through which the IHS are formed [26,27].

3.1. Physical Crosslinking

In hydrogels that physically crosslink, the crosslinking is processed by noncovalent bonds. Physical crosslinking involves, e.g., electrostatic interactions (ionic and hydrogen bonding), host–guest interactions, and hydrophobic interactions. IHS produced by physical crosslinking in response to exposure to physical, photoinitiator, or chemical stimuli are usually reversible and display responsiveness to stimuli [20,28].

3.1.1. H-Bonding

Hydrogen bonding has been promised as a common crosslinking strategy since it can provide the possibility to prepare IHS with thermoelectricity and self-healing properties at the same time [29–31]. IHS can be formed in response to the H-bonding between the different functional groups (OH, CO₂H, SO₃H, or NH₂, etc.) along the polymeric chains [32,33]. For example, chitosan modified with adamantane (AD) underwent self-crosslinking through the formation of inter-chains hydrogen bonding [34]. Geng et al. [32] developed injectable, sprayable, and hemostatic hydrogels by mixing tannic acid (TA) and *O*-carboxymethyl chitosan (CMCS) at different ratios; the hydrogel was spontaneously formed without an external stimulus, in particular in the presence of benzene boronic acid (BDBA) (Figure 3). The CMCS–TA–BDBA hydrogel is assembled via hydrogen bonds between TA and CMCS; meanwhile, BDBA forms dynamic boronate ester bonds with TA. The resulting CMC-based IH displays a rapid gelation rate (~10 s) and self-healing ability within 12 h at 25 °C. Moreover, the hydrogel demonstrated a biocompatibility profile when tested against MCF-7 human breast cancer cells.

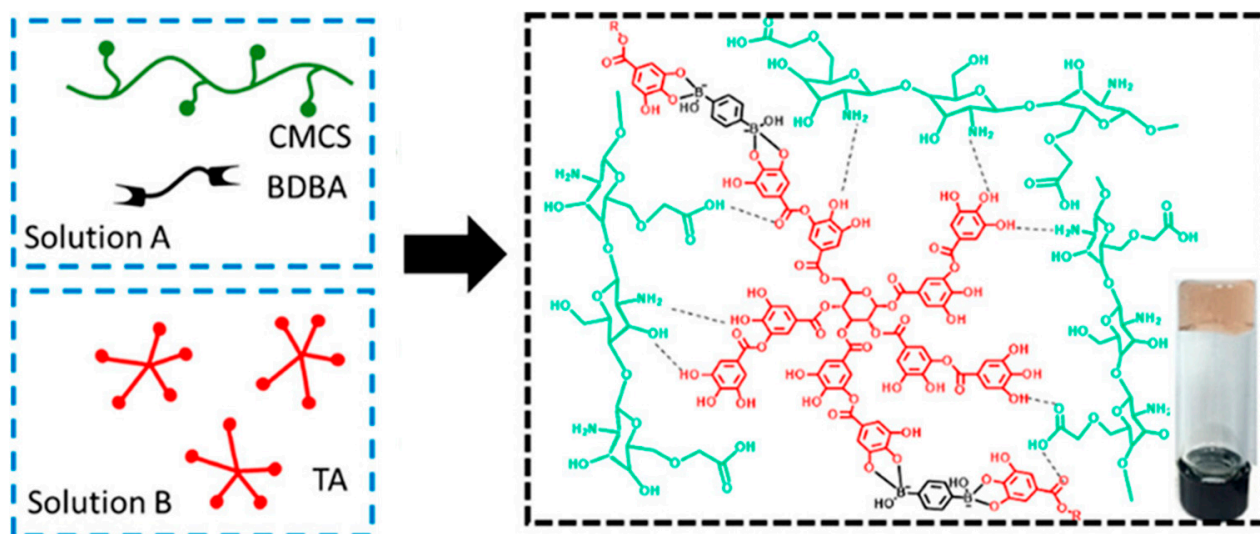


Figure 3. Formation of CMCS–TA–BDDBA hydrogel via hydrogen bonding and boronate ester bonds with TA (adapted with permission from Geng et al., 2020).

3.1.2. Hydrophobic Interactions

This crosslinking approach is commonly used for the preparation of reversible IHs. This mechanism works for amphiphilic polymers, which contain hydrophobic moieties (gelators) that gelate upon increasing the temperature [35–37]. For example, Hsiao et al. [38] reported the development of self-assembled injectable nanogels using amphiphilic carboxymethyl-hexanoyl chitosan (CHC) with glycerophosphate disodium salt. The resulting nanogel was employed as a drug delivery carrier to control the delivery of Genipin. In another study, Lu et al. [39] prepared pH-responsive in situ injectable hydrogels to encapsulate berberine. The hydrogel was formed by blending carboxymethyl hexanoyl chitosan (CHC) with low molecular weight hyaluronic acid (LMW HA). The formed nanoparticles self-assembled into injectable hydrogels by stirring (Figure 4). The hydrogel sustained the release of berberine at pH 6.0 (simulating inflamed arthritic articular cartilage). Moreover, the hydrogel showed biocompatibility when protecting the chondrocytes against sodium nitroprusside-induced apoptosis. Moreover, the gels demonstrated slower biodegradation rates between pH 5.0 and 6.0 compared to pH 7.4.

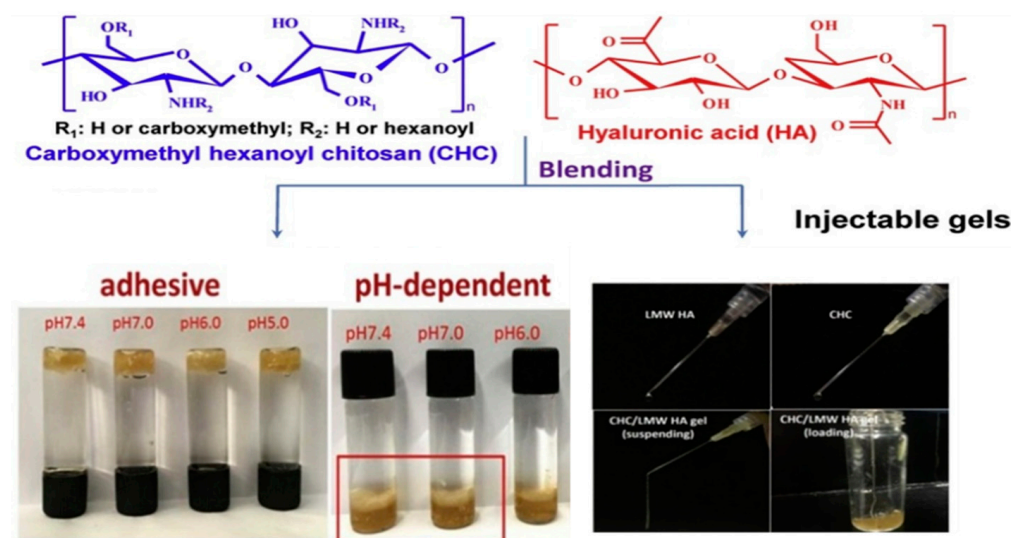


Figure 4. Preparation of CHC/HA IHs via hydrophobic interaction (adapted with permission from Lu et al., 2019).

3.1.3. Ionic Interactions

Ionic crosslinking between oppositely charged polymers (polyelectrolytes); cationic polymers, e.g., chitosan polyethylenimine (PEI), with anionic polymers, e.g., sodium alginate, carrageenan, tannic acid, chondroitin sulfate) [37]. In this type of IHs, the rate of hydrogel injectability depends on the pH, the ratio between the oppositely charged precursors, and temperature. For example, blending chitosan quaternary ammonium salt and anionic sodium alginate generated a dual crosslinking hydrogel with excellent injectability. The formed hydrogel showed a uniform 3D network structure, robust mechanical properties, and good biocompatibility toward NIH-3T3 cells [40]. The injectable hydrogel formed due to ionic interaction and hydrogen bonding between carrageenan, locust bean gum, and gelatin successfully accelerated the *in vitro* wound healing in HUVEC cells and tissue repairing [41]. Chen et al. fabricated a high-strength, tough, and self-healable IHs by grafting poly (acrylic acid) into carboxymethyl cellulose (CMC), followed by crosslinking with Fe^{3+} ions [42]. Similarly, the IHs prepared by ionic crosslinking of κ -carrageenan with chitosan/nanohydroxyapatite were used as a platform to sustain the release of ciprofloxacin (Figure 5) [43].

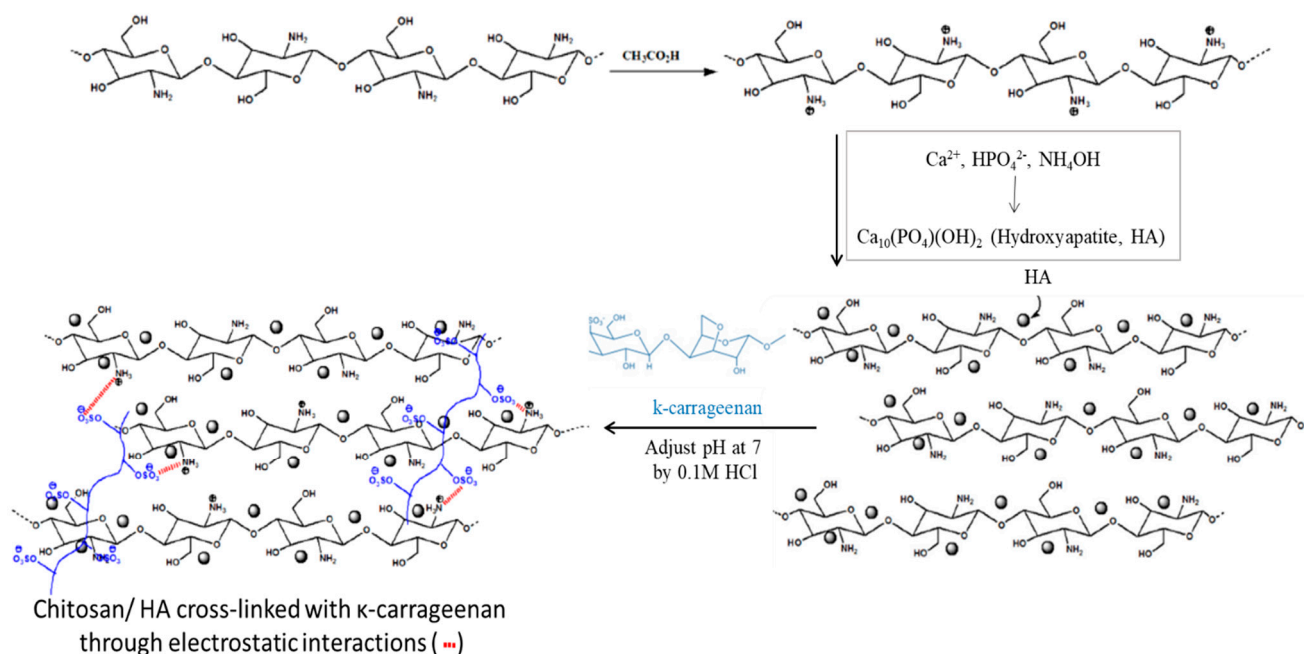


Figure 5. Preparation of κ -carrageenan-crosslinked chitosan/nanohydroxyapatite hydrogel via ionic interaction (adapted with permission from Mahdavinia et al., 2019).

3.1.4. Host–Guest Interaction (Inclusion Mechanism)

In this mechanism, one molecule has a cavity (host). Inside this cavity, the other molecule (guest) is embedded. Macrocyclic compounds (e.g., cyclodextrins (CDs), calixarenes, and cucurbit[n]urils), crown ethers, catenanes, cyclophanes, pillararene, cryptophanes, and porphyrins) demonstrated potential efficiency as the host for inclusion complexation [44–46]. These macrocycles have unique internal and external properties that can capture guest molecules and form inclusion complexes in the solvent [47]. Cyclodextrins (CDs) have a hydrophobic inner cavity and can host hydrophobic guest molecules such as adamantane (Ad), azobenzene, etc. [48,49]. In this regard, Okubo et al. [50] innovated thermoresponsive IHs based on the interactions between various cyclodextrins (CD) and stearate-modified hydroxypropyl methylcellulose (HM-HPMC) through the inclusion mechanism (HM-HPMC/ β -CD). Based on the thermoresponsive sol-gel transition property, the appropriate formulation was selected and studied for its ability to encapsulate and control the release of insulin, a model drug, from the hydrogel after subcutaneous administration. In another attempt, the host–guest inclusion complexation between polymerized

β -cyclodextrin (CDP) and adamantane-conjugated Pluronic F127 (F127-Ad) developed self-assembly thermoreversible, micels such as IHs as well, as shown in Figure 6. The hydrogel revealed *in vitro* and *in vivo* long-term stability for up to 30 days and endowed the sustained release of insulin and gelatin [51].

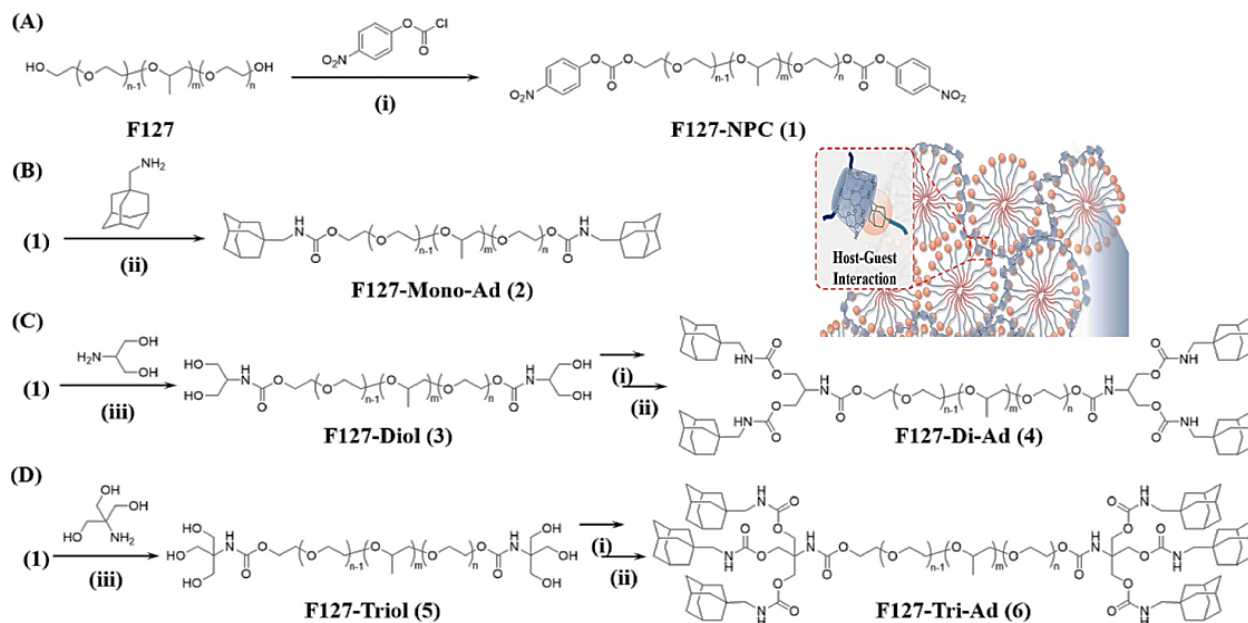


Figure 6. Synthetic (A) F127-NPC, (B) F127-Mono-Ad, (C) F127-Di-Ad, and (D) F127-Tri-Ad. and host-guest interaction with β -cyclodextrin, which assembles into micells (adapted with permission from Lee et al., 2021).

3.2. Chemical Crosslinking

The injectable hydrogel is formed in the chemical crosslinking approach due to covalent bonds between the polymeric chains [21]. Michael-type addition, click reactions, disulfide linkage, photopolymerization, hydrazone, and imine-linkages are involved in the formation of reversible covalent bonds and formation of injectable hydrogels. The chemical coupling and hydrogel formation are usually initiated upon the addition of nucleophile-bearing small molecules or polymers with proper functionality. The chemical crosslinking is generally triggered by external physical stimuli such as photoinitiation, heat, pH change, or enzymatic reactions to induce the slinking between the polymeric chains [52]. Unlike physical crosslinking, covalent crosslinking is more stable, especially in physiological conditions, giving chemical crosslinking preference over physical crosslinking in controlling drug release [34,37].

3.2.1. Schiff Base Coupling Reactions

The reaction between a primary amine-containing polymer or small molecule and an aldehyde-containing polymer or small molecule results in the formation of reversible imine, hydrazone, or oxime linkages (Schiff base bonding). Besides, the reaction is highly selective and can process very smoothly at a fast rate without using a hazardous catalyst. Therefore, the hydrogel can recover its integrity and shape if exposed to surface disruption by an external force. In addition, the Schiff base or acyl hydrazone bonds are stable in the neutral and alkaline pH, but they are easily hydrolyzed in acidic conditions at pH 5 or less [53]. The well-known example of such a mechanism is the crosslinking of chitosan by glutaraldehyde [54,55]. Moreover, because the imine and hydrazone linkages-based IHs have the advantages of self-healing, sensitivity, and response to the pH changes, they are potentially utilized as site-selective platforms for the smart localization and release of different therapeutic agents [53,56,57], cell therapy [58,59], tissue regeneration [60,61], and dressings for wounds [62–66]. As a representative example, the preparation of injectable

hydrogels and their application as antibacterial, self-healing, and adhesive biocompatible wound dressings were presented by Chen et al. [67]. Chen and his colleagues developed a series of multifeatured injectable e-hydrogels via the imine linking between oxidized konjac glucomannan and chitosan-free amine groups. The resulting hydrogels were 100% cytocompatible with L929 fibroblasts, even after 72 h incubation. Additionally, the hydrogel demonstrated a remarkable ability in promoting the wound healing and inhibiting the growth of *Staphylococcus aureus* and *Escherichia* by 96 and 98%, respectively [67]. In another example, when the dialdehyde hydroxyethyl starch (AHES) condensed with both doxorubicin (Dox) and the tumor homing cyclic RGD peptide [68] with the sequence cyclo(Arg-Gly-Asp-d-Phe-Lys), it produced a dual-targeting-IH. The hydrogel selectively localized Dox to the $\alpha\beta$ -integrin receptor-over-expressing malignant melanoma (A375 cells) and controlled its release in a pH-responsive manner (Figure 7) [69].

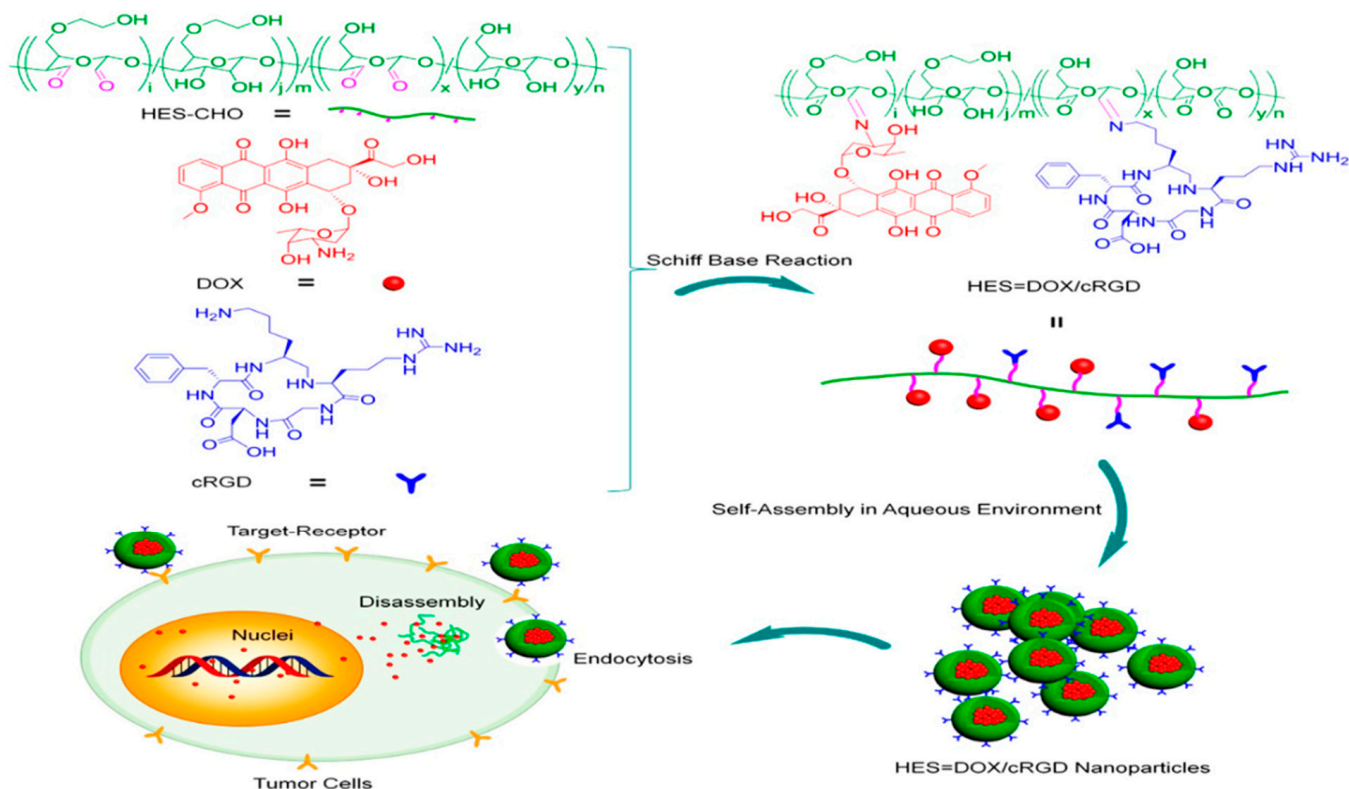


Figure 7. Schematic representation for coupling of dialdehyde hydroxyethyl starch with cyclo(Arg-Gly-Asp-d-Phe-Lys) and Dox via Schiff base reaction for selective localization and pH-dependent release of Dox.

The properties of hydrazone crosslinked hydrogels can be controlled by the number of crosslinkable groups, the molecular weight of the polymer, the ratio of gel components, and water content. Likewise, When dialdehyde gullen gum (GG) reacted with hyaluronic acid (HA) modified adipic acid dihydrazide, it produced hydrazone crosslinked hydrogels. The GG-HA-hydrogels demonstrated controllable injectability, swelling, and biodegradation rates, as well as tunable rheological properties, supporting their use in regenerative medicine (Figure 8) [70].

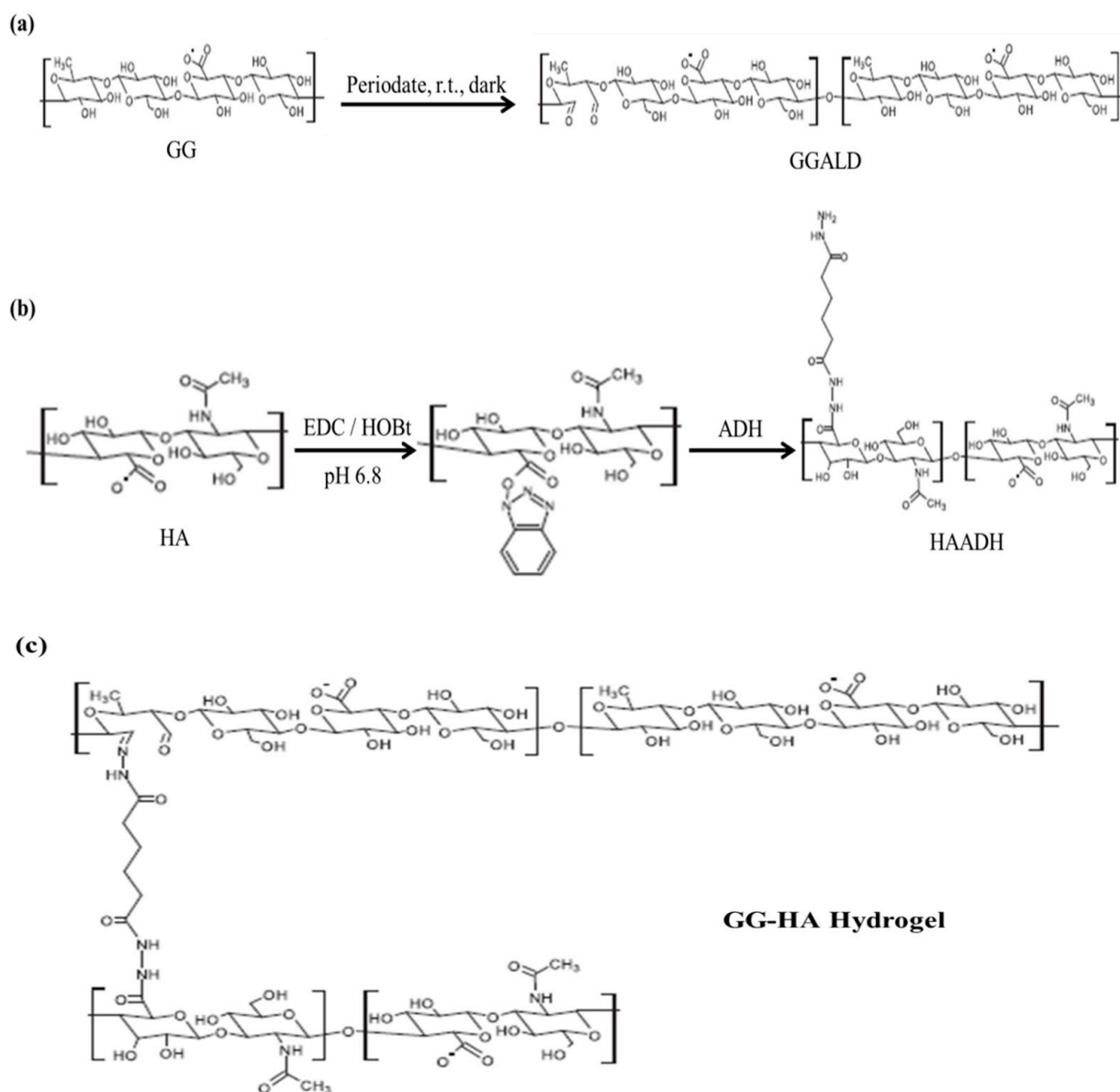


Figure 8. (a) Aldehyde-modification of GG (GGALD), (b) hydrazide-modification of HA (HAADH), and (c) The chemical structure of hydrazone crosslinked GG-HA hydrogels (adapted with permission from Karvinen et al., 2018).

3.2.2. Michael-Type Addition Reactions

Michael-type addition reaction is a thermodynamic nucleophilic addition reaction to α ,-unsaturated carbonyl linker. These α ,-unsaturated carbonyl compounds involve the nucleophilic addition reaction between carbanion of nucleophile-bearing polymers, such as thiols or amines bearing polymers or molecules and polymer functionalized with α , β -unsaturated carbonyl linker. The development of an injectable in situ forming hydrogel using the azo-type Michael reaction between amine-decorated hyaluronic acid and vinylsulfone functionalized β -cyclodextrins encapsulating doxorubicin [71] in an aqueous environment at 37 °C. The hydrogel sustained the release of Dox and inhibited the proliferation of 3D cultured-colorectal carcinoma in vitro and drastically reduced the xenograft of human colon carcinoma in vivo without cytotoxic side effects on the heart (Figure 9). Additionally, thiolated dextran (Dex-SH) with a degree of substitution of 10 was synthesized and used for in situ hydrogels formation with vinyl sulfone functionalized Pluronic 127 (PL-VS) or acrylate Pluronic 127 (PL-Ar). The dextran/pluronic hydrogels were formed under physiological conditions upon mixing. The rheological studies showed that these

hydrogels with a broad range of storage moduli of 0.3–80 kPa could be obtained by varying the concentration of PL-VS or PL-Ar from 5 to 20% (*w/v*). [72]. When thiolated glycol chitosan (GCH-SH) and vinyl sulfone-modified PEG (PL-VS) were mixed, the in situ IHs were formed under physiological conditions and successfully applied as biodegradable, non-toxic scaffolds for cartilage regeneration [73].

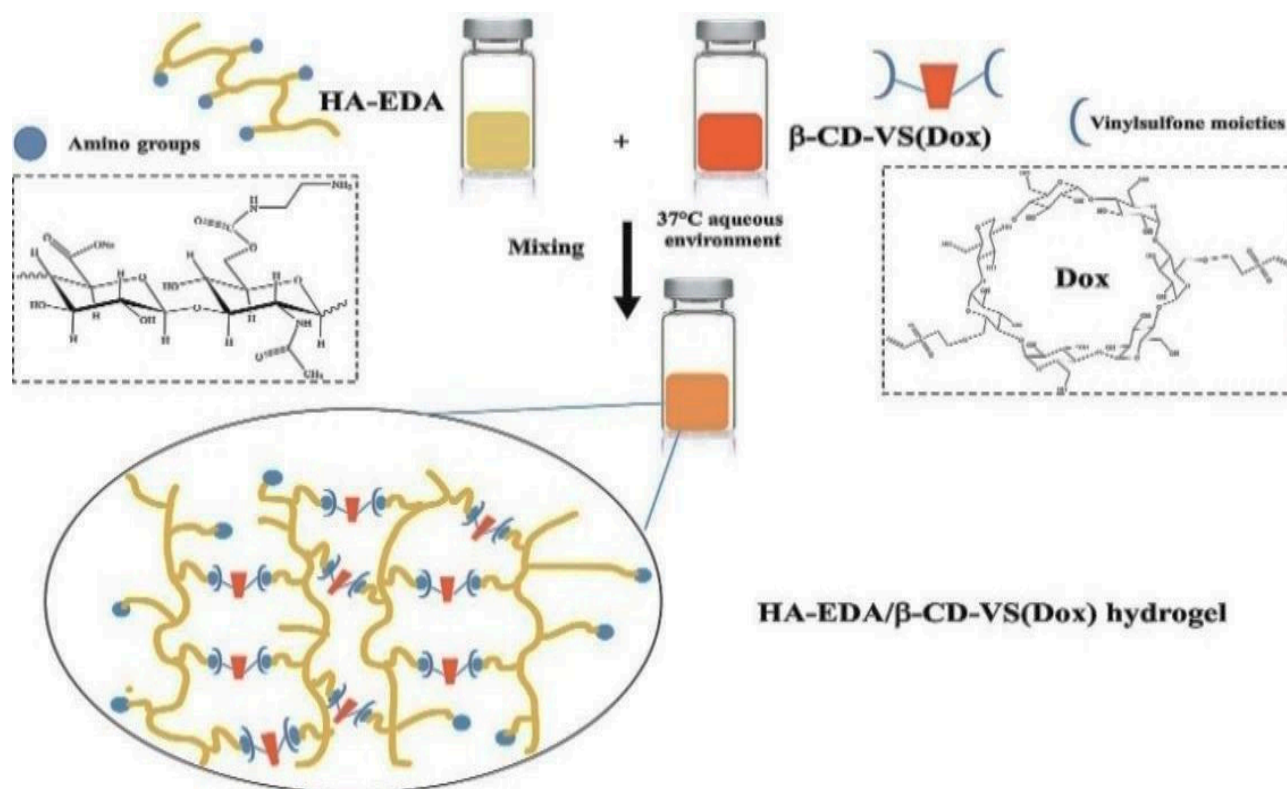


Figure 9. Schematic representation for the preparation of injectable hydrogel via azo-type Michael reaction between HA-EDA and β -CD-VS(Dox) (adapted with permission from Fiorica et al., 2021).

3.2.3. Disulfide Bridge

The disulfide bonds are formed by the reaction of thiol groups in the polymer chains to form disulfide bonds in a mild oxidative environment [74]. The process of thiol oxidation depends on the number of thiolate anions and the change in the pH [75]. For instance, the coupling of *N*-acetyl-cysteine (NAC) to chitosan-*g*-poly *N*-isopropylacrylamide (CS-*g*-PNIAM) and oxidation of the thiol groups under mild conditions resulted in the formation of temperature-sensitive, pH-responsive IHs with improved mechanical properties compared to non-crosslinked CS-*g*-PNIAM hydrogel (Figure 10) [76]. A series of injectable hydrogels were prepared via in situ disulfide bridge formation between cysteamine-modified hyaluronic acid and carboxymethyl cellulose at 37 °C, without any chemical additive. The crosslinking between hyaluronic acid and carboxymethyl cellulose took place within 1.4–7.0 min, and the resulting hydrogels displayed superior rheological properties, a high swelling ratio, good stability, and a sustained release rate for bovine serum albumin (BSA) [77].

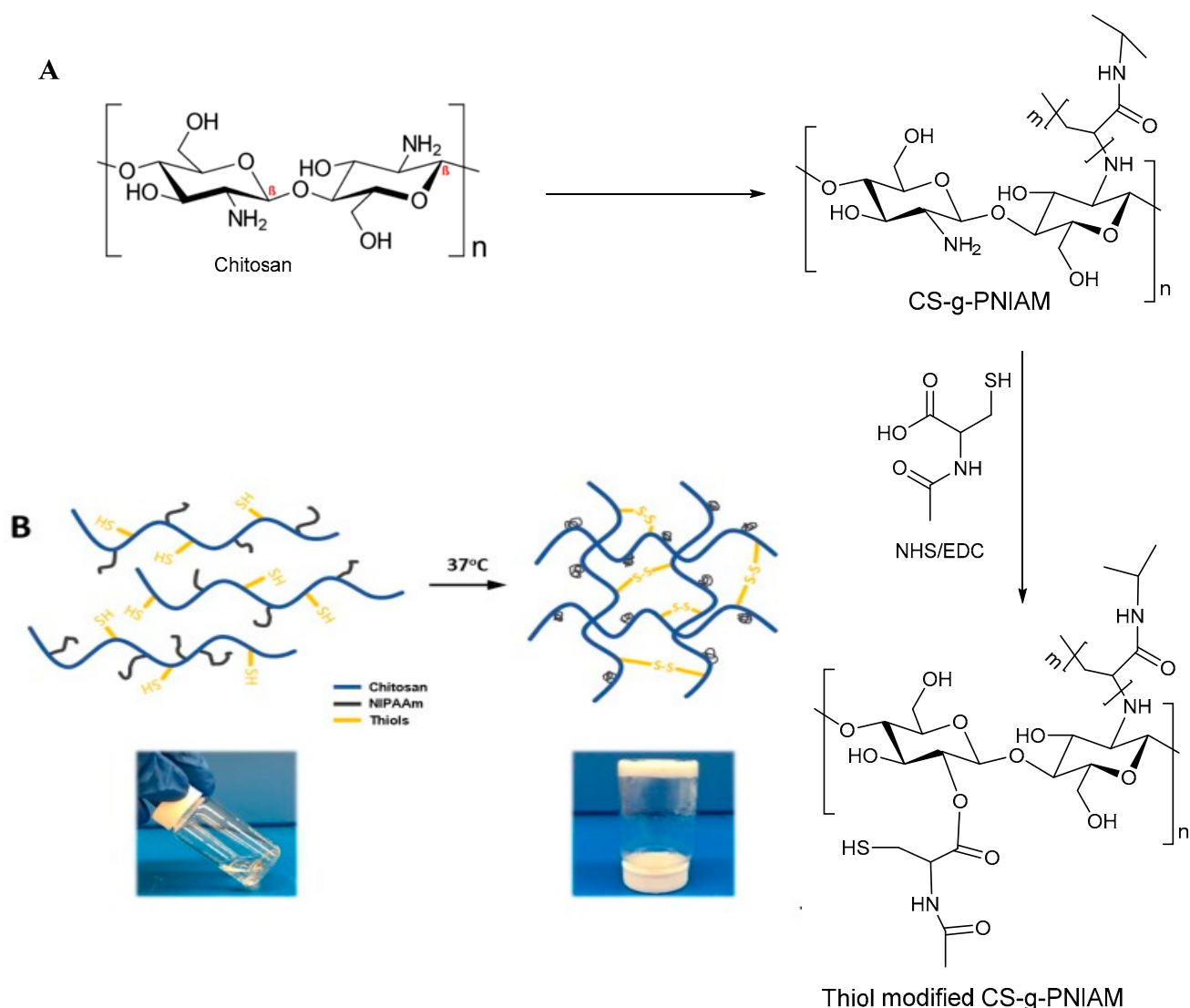


Figure 10. Formation of IHs via disulfide bonds between the free thiol containing polysaccharide polymers. (A) copolymerization of N-isopropylacrylamide with chitosan and thiol modification using carbodiimide (B) gelation mechanism; physical (helix-coil structure) and chemical cross-linking (disulfide bond formation) (adapted with permission from Wu et al., 2018).

3.2.4. Crosslinking via Click Chemistry

Click chemistry is defined as the chemical reactions that take place spontaneously between two different reactants at the mild condition in a highly selective manner affording high product yields. This method includes different sub-categories such as alkyne-azide click reactions, Diels–Alder (DA), cycloaddition, and thiolene addition reactions [78–80].

Alkyne–Azide

Cu(I)-catalyzed click reaction between molecule carrying azide end and terminal acetylene moieties from another molecule forming 1,2,3-triazoles ring is an example of click chemistry. This reaction has attracted attention because it can be achieved in mild conditions with high substrate selectivity [81]. In this context, J. Zhang and his research colleagues prepared a series of thermosensitive P(NIPAAm-*co*-HEMA)/cellulose hydrogels [82]. The hydrogels were fabricated in situ upon simple mixing of alkyne-modified cellulose and poly(*N*-isopropylacrylamide-*co*-hydroxyethyl methacrylate), (Figure 11).

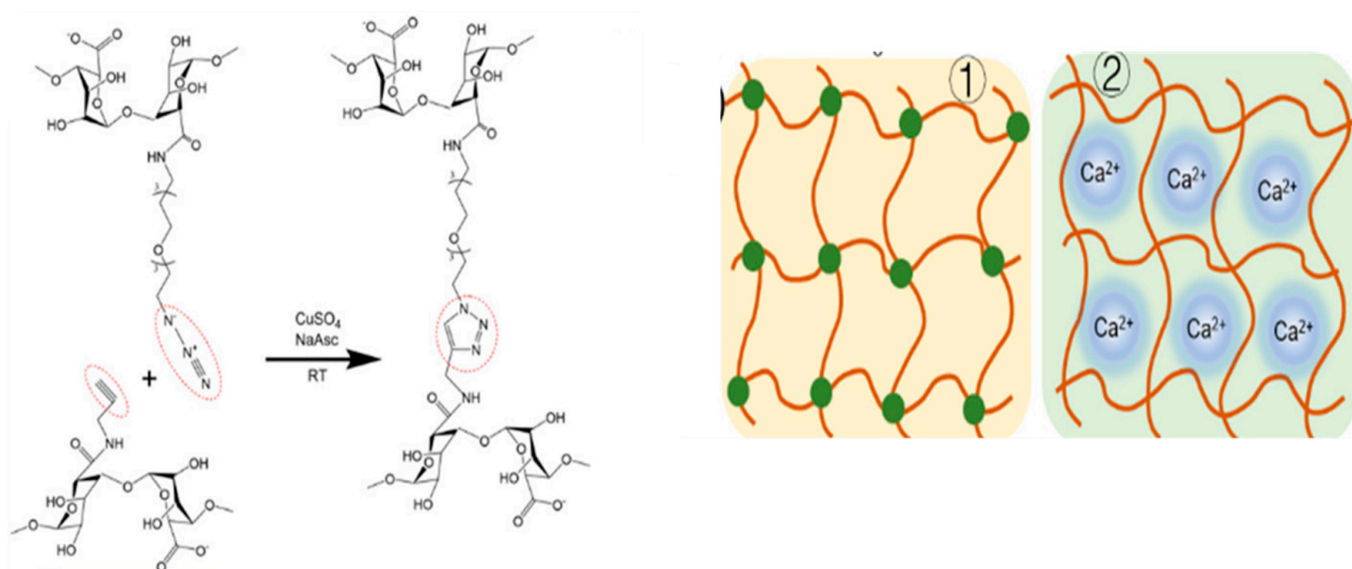


Figure 11. Schematic illustration for the Cu(I)-mediated cross-linking between P(NIPAAm-co-HEMA) and cellulose (adapted with permission from Zhang et al., 2009).

Diels–Alder (DA)

The Diels–Alder crosslinking between furan-modified pectin (PF) and maleimide-modified chitosan (CA) introduced a multifunctional platform that has been employed in the suitable and selective delivery of 5-fluorouracil. Hence, the hydrogel showed self-healing ability at 37 °C for 5 h. The cytotoxicity of the resultant hydrogels was found to be 90 after 24 h of cell culture and 80% after 72 h of incubation with mouse fibroblasts (L929). The 5-FU loading efficiency was found to be 53.67–65.27%, while its release rate increased by increasing the pH value (Figure 12) [83].

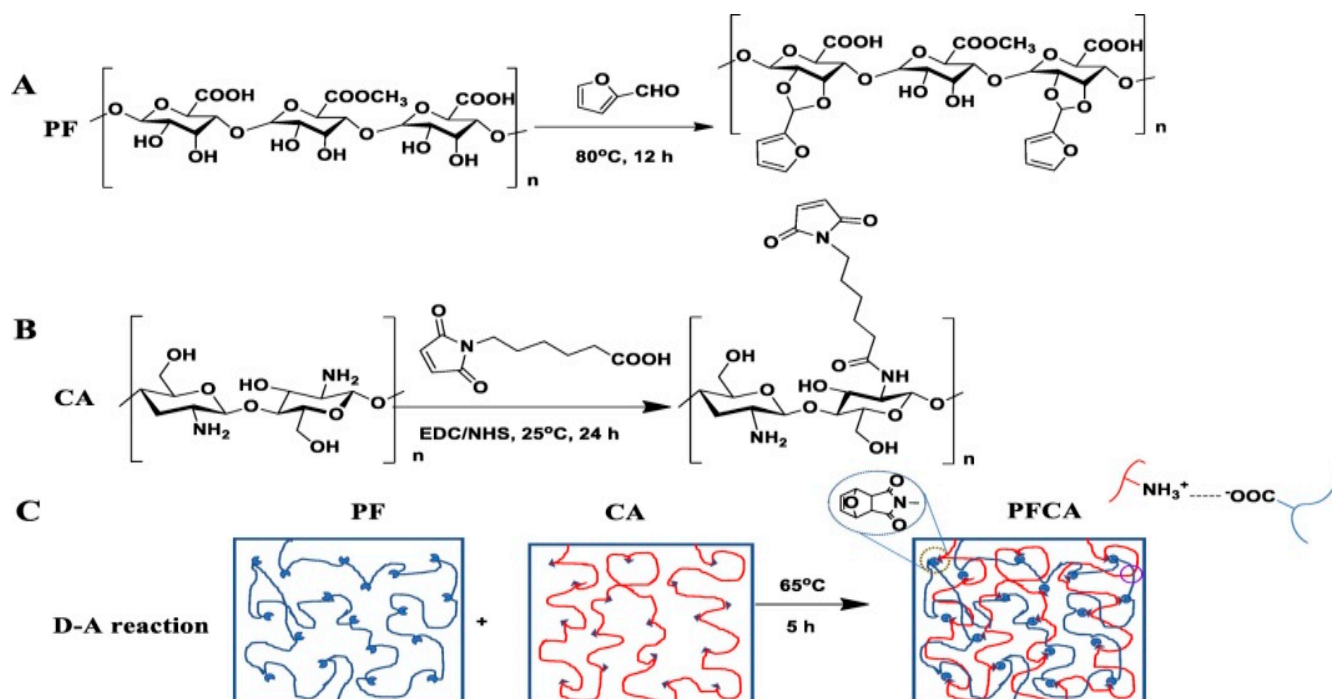


Figure 12. (A) modification of pectin with furan, (B) modification of chitosan with maleimide, and (C) the D-A reaction between furan-modified pectin (PF) and maleimide-modified chitosan (CA) forming in situ hydrogel (adapted with permission from Le et al., 2021).

Cycloaddition

An injectable hydrogel was prepared via the click-crosslinking of hyaluronic acid (HA) modified with a bone morphogenetic protein-2 (BMP-2) and mimetic peptide (BP). The hydrogel was employed as a scaffold for bone tissue engineering. The scaffold was prepared simply by mixing HA-Tet and HA modified with cyclooctene-amine. The hydrogel scaffold was stable for a longer period than HA both in vitro and in vivo, and provided a biocompatible environment for the osteogenic differentiation of loaded hDPSC [84]. The hydrogel formulation was prepared from HA-tetrazine (HA-Tet) and HA-cyclooctene (HA-TCO). The scaffold was prepared simply by mixing HA-Tet and HA-TCO. The Cx-HA hydrogel scaffold was stable for a longer period than HA both in vitro and in vivo, which was verified via in vivo fluorescence imaging in real-time. BP acts as an osteogenic differentiation factor for human dental pulp stem cells (hDPSCs). After its formation in vivo, the Cx-HA scaffold provided a good environment for the hDPSCs, and the biocompatibility of the hydrogel scaffold with tissue was good. Like traditional BMP-2, BP induced the osteogenic differentiation of hDPSCs in vitro. The physical properties and injectability of the chemically loaded BP for the Cx-HA hydrogel (Cx-HA-BP) were nearly identical to those of the physically loaded BP hydrogels, and the Cx-HA-BP formulation quickly formed a hydrogel scaffold in vivo. The chemically loaded hydrogel scaffold retained the BP for over a month. The Cx-HA-BP hydrogel was better at inducing the osteogenic differentiation of loaded hDPSCs because it prolonged the availability of BP. In summary, They successfully developed an injectable, click-crosslinking Cx-HA hydrogel scaffold to prolong the availability of BP for efficient bone tissue engineering (Figure 13) [84].

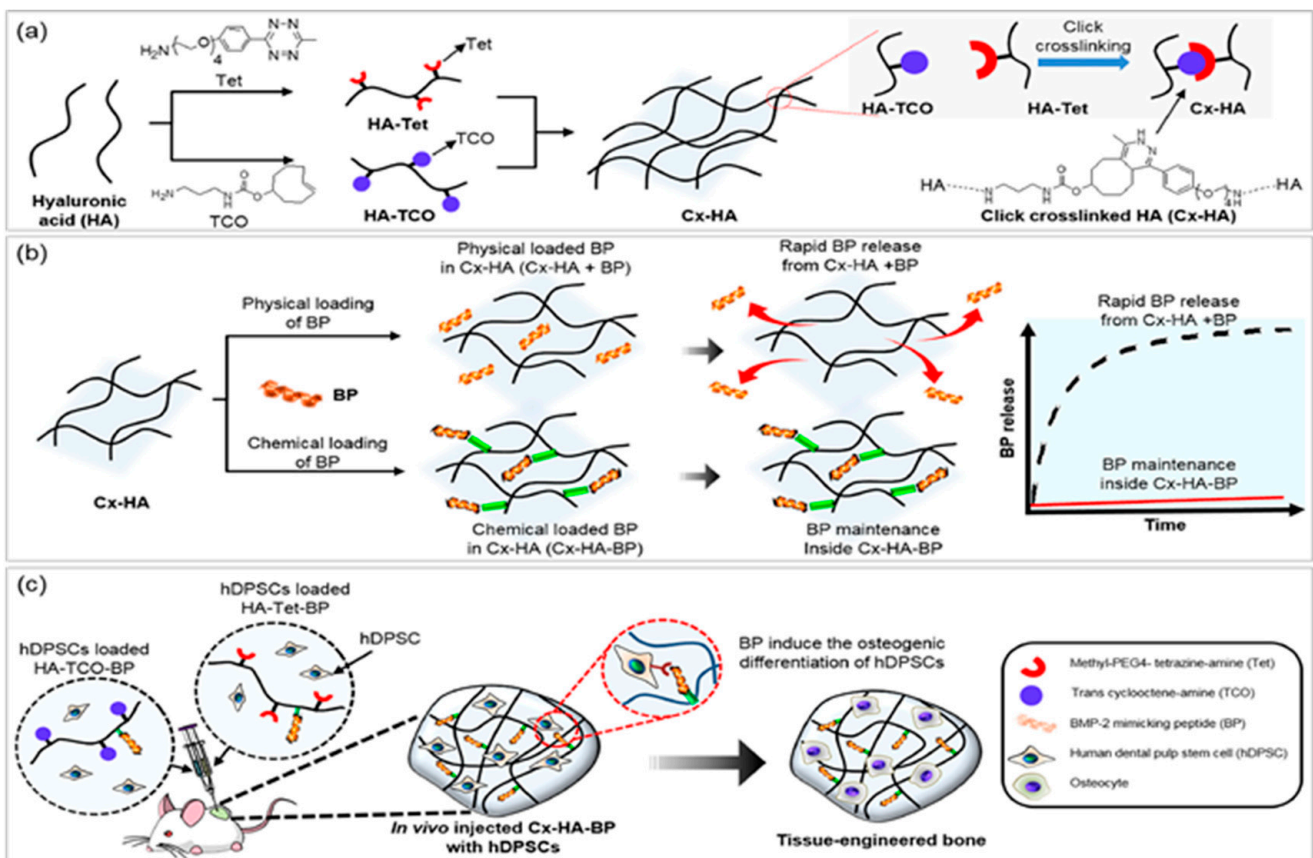


Figure 13. Schematic illustration for the preparation of (a) HA-Tet, HA-TCO, and Cx-HA (b) the release pattern for of BP from Cx-HA(+BP) and Cx-HA-BP; (c) osteogenic differentiation of hDPSCs on Cx-HA-BP (adapted with permission from Zhang et al., 2012).

Thiolene Addition

Q. Wang et al. [85], utilized thiolated cellulose nanocrystal (CNC-SH) as a nanofiller and crosslinker for a 2% methacrylate-modified *O*-acetyl-galactoglucomanan (GGMMA) hydrogel. CNC was isolated from the microcrystalline cellulose and oxidized to dialdehyde CNC coupled to cystein via imine linkages, which was followed by reductive amination to generate the corresponding CNC-SH. The photo-initiated thiol-ene addition between GGMMA and CNC-SH offered a high-efficacy photo-curable, interpenetrating, and injectable hydrogel (Figure 14). The bioactive glass nanoparticle (BaGNP) was embedded and loaded into the GGMMA/CNC-SH hydrogels, resulting in the sustained release of Si and Ca ions in simulated body fluid *in vitro*.

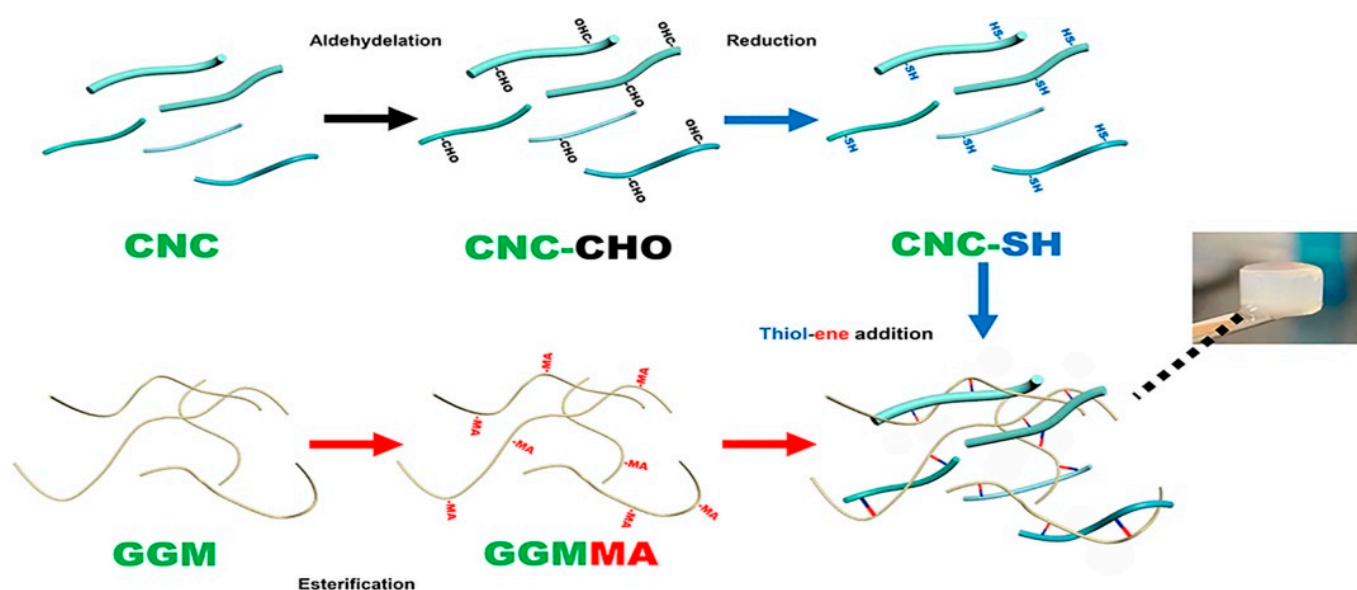


Figure 14. Fabrication of GGMMA/CNC-SH hydrogel via photo-initiated thiol-ene addition between GGMMA and CNC-SH (adapted with permission from Wang et al., 2022).

3.3. Enzyme-Mediated Reaction

Several research groups have studied the preparation of IHs through enzyme-mediated crosslinking [86,87]. Hydrogen peroxide (H_2O_2) and horseradish peroxidase (HRP) enzymes are usually used to mediate the gelation process, which could be formed within a few seconds to minutes by varying the concentration of H_2O_2 and HRP [88,89]. In this context, a series of dopamine-modified carboxymethyl cellulose (CMC-DA) biodegradable IHs was prepared by *in situ* enzymatic crosslinking in the presence of HRP and H_2O_2 . The CMC-DA hydrogel demonstrated, *in vitro*, good cytocompatibility against BMSC (with viability over 90% within 5 days of culture) when evaluated using the three-dimensional culture method. Moreover, The strong tissue adhesive ability offered by the hydrogel was about 6-fold over the commercial fibrin glue promising their application as tissue adhesive material [90]. Moreover, when hyaluronic acid conjugated tyramine (HA-TA) and chondroitin sulfate-tyramine (CS-TA) crosslinked using HRP/ H_2O_2 , the IHs were obtained within 15 s. The hydrogel was used for *in situ* encapsulation of mesenchymal stem cells (BMSCs) and bone morphogenetic protein-2 (BMP2) [91]. Since the use of a high concentration of H_2O_2 to catalyze the crosslinking reaction leads to the formation of heterogeneous hydrogels, L. Wang et al. [92] designed a new method for the horseradish peroxidase-mediated hyaluronic acid gel with tyramine. According to his method, galactose oxidase (GalOX) was employed to catalyze the controlled production of H_2O_2 (Figure 15). This new tyramine-modified hyaluronic acid (HT) hydrogel exhibited good injectability, favorable cytocompatibility, and efficiency in the encapsulation of bone marrow mesenchymal stem cells (BMSCs), with a minor inflammatory response. The gelation time,

swelling behavior, and degradation rate of the HT hydrogel could be modified by varying the concentrations of HA and GalOX within a certain range.

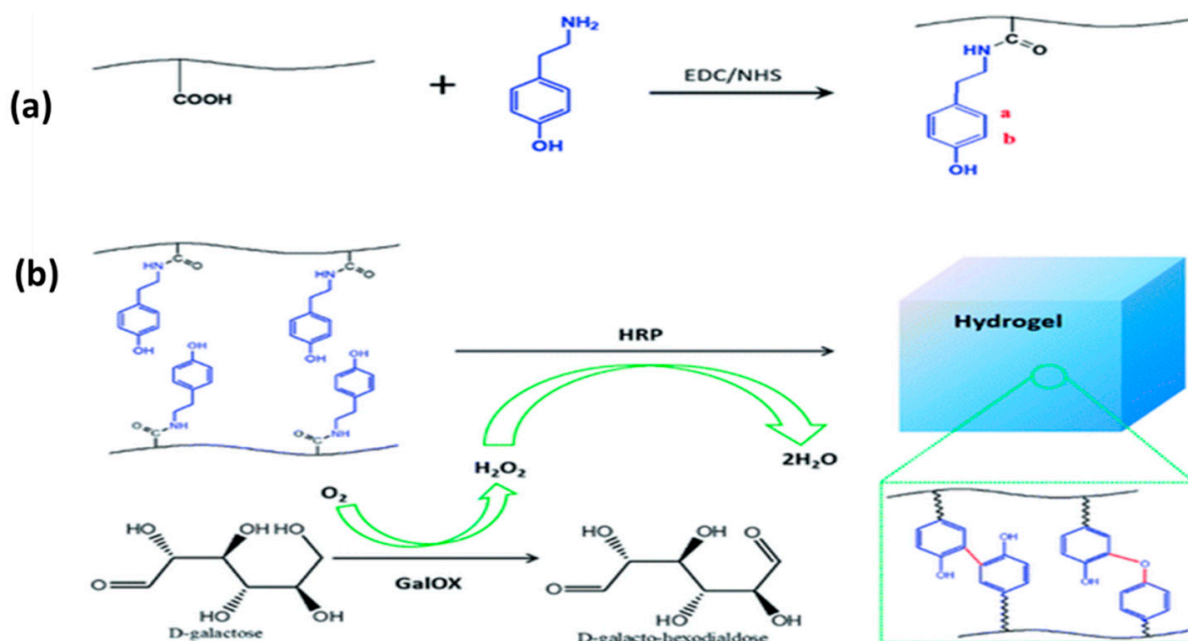


Figure 15. Synthetic scheme of; (a) the hyaluronic acid–tyramine (HT) conjugate and (b) hydrogel formation by dual-enzymatically crosslinked HRP and GalOX (adapted with permission from Wang et al., 2020).

3.4. Photo Initiation

In this mechanism, the crosslink is simultaneously initiated by visible or ultraviolet (UV) light for the hydrogel precursor bearing a methacrylate moiety in the presence of the initiator [18]. In some cases, photo-crosslinking can be used as a second strategy for gelation to improve the mechanical properties and stability of the IHs [93,94]. The low penetration rate of UV light onto the polymer mixture is the major disadvantage of this mechanism. Therefore, visible light has been used instead of UV light to ensure a higher penetration ability and lesser damage to the tissue [95,96]. H. Zhao et al. [97] developed hyaluronic acid (HA)/cellulose nanofiber (CNF) nanocomposite hydrogels by photo crosslinking between methacrylated CNFs and methacrylated HA in the presence of lithium phenyl (2,4,6-trimethylbenzoyl) phosphinate (LAP) as a photoinitiator. The hydrogel offered in vitro good microenvironment that enhanced the bone marrow mesenchymal stem cells (BMSCs) survival and proliferation. Meanwhile, the dual crosslinking strategy was employed to convert dopamine-modified hyaluronic acid (HA-DA) into the injectable hydrogel. The black phosphorous nanosheets loaded with a Zr-based porphyrinic metal–organic framework (PCN@BP) were integrated into the hydrogel and initiated the photo-oxidative coupling of dopamine by generating reactive oxygen species (ROS) under 660 nm laser irradiation [86]. L. Wang and his collaborators [98], fabricated a series of IHs with interpenetrating, adhesive, wounds healing, and hemostatic anti-bacterial properties by dual crosslinking strategy. The first layer of the hydrogel was assembled between catechol-modified methacryloyl chitosan and methacryloyl chitosan through catechol/Fe³⁺ chelation. Then, the second layer of crosslinking was achieved by the photopolymerization of methacrylate along the chitosan chain. This dual crosslinking plane for chitosan enhanced the hydrogel compressive modulus and ductility, as illustrated in Figure 16.

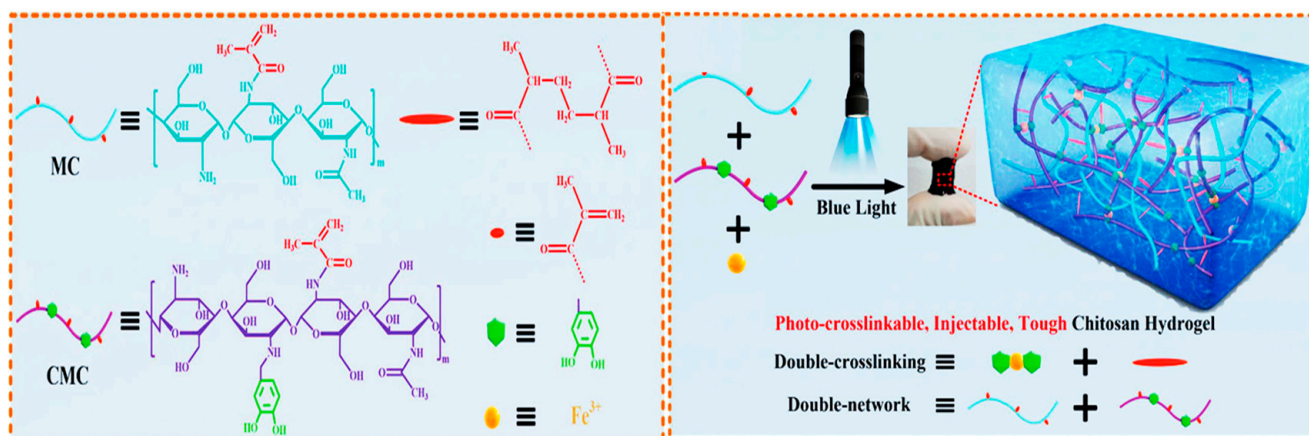


Figure 16. Schematic illustration on the fabrication of a photo-crosslinkable, injectable chitosan-based hydrogel with enhanced tissue adhesion and antibacterial activity.

4. Biomedical Applications of Polysaccharides-Based Injectable Hydrogels (PSIHs)

IHs prepared by using one or more polysaccharides offer the advantage of their ability to simulate an environment that more or less mimics the extracellular matrix (ECM) and can support the cell's migration, growth, and proliferation. Therefore, PSIHs have received immense attention for their applications in regenerative medicine and tissue engineering. In addition, polysaccharide polymers are rich in different types of functional groups that enable further modification and crosslinking to impart novel features to the resulting hydrogels for a wide range of uses in biomedical and regenerative medicine.

4.1. Delivery of Chemotherapeutics

The major problem of current delivery systems is the non-selective and the burst or the delayed release of therapeutic agents from the matrix [99], resulting in a reduction of the therapeutic efficacy of the drug as well as undesirable biodistribution and organ toxicity [100,101]. On the other hand, several approaches have been investigated to achieve selective drug delivery [102,103] and control their release pattern [104,105]. The interest in stimuli-responsive IHs as a delivery vehicle for different biologically active molecules has been significantly growing over the last decade [106,107] due to their rapid response to external stimulus and the capability to homogeneously integrate the active ingredients within the hydrogel precursors before injection [108–111]. In addition, the encapsulation of the active therapeutic does not need harsh conditions that may affect the drug stability. Moreover, IHs can be molded *in vivo* using a double-barrel syringe to extrude the hydrogel components directly to the desired location [112]. Qu et al. reported the encapsulation of Doxorubicin (Dox) into the IHs formed through dynamic covalent Schiff-base linkage between *N*-carboxyethyl chitosan (CEC) crosslinked with dibenzaldehyde-terminated poly(ethylene glycol) (PEGDA). The PEGylated chitosan-based IHs had excellent cytocompatibility on L929 cells and controlled the Dox release in pH-responsive pattern. Moreover, the Dox released from the hydrogel dramatically inhibited the proliferation of HepG2 cells at a concentration lower than 0.1 $\mu\text{g}/\text{mL}$ compared to the untreated cells. When the Dox concentration in the hydrogel increased from 0.1 to 0.25 $\mu\text{g}/\text{mL}$, its antiproliferative potency against HepG2 cells was as efficient as that of free Dox. These *in vitro* findings were further confirmed by the confocal microscopy study that showed the amount of live and dead cells was proportional to the Dox concentration in the hydrogel [113]. Another attempt to encapsulate and control the release of Dox was attained by its encapsulation into an injectable composite hydrogel formulated via the hydrazone crosslinking between hydrazide-modified carboxymethyl cellulose (CMC-NH₂) and dialdehyde carboxymethyl cellulose (CMC-CHO) containing poly(ethylene oxide)-block-poly(2-(diisopropylamino) ethyl methacrylate) (PEO-b-PDPA) copolymers micelles. The IHs exhibited tunable degra-

dation properties, pH sensitivity, and prolonged the release of Nile Red dye and Dox drug [114].

On the other hand, PSIHs have been employed for the encapsulation and localization of water-insoluble drugs such as curcumin [115–117]. For example, the encapsulation and localization of curcumin into a novel IHs developed by simple Michael addition crosslinking strategy between thioglycolic acid decorated chitosan (TCS) and poly(ethylene glycol) diacrylate (PEGDA). The inactivated starch-coated lysozymes (α -amylase and glucoamylase) were encapsulated into the hydrogel to increase the rate of the drug release from the hydrogel and improve the anti-tumor activity. The in vivo anticancer activity in HEPG2 tumor-bearing nude mice revealed the ability of the hydrogel system to effectively slow down tumor growth and induce selective apoptosis in the tumor cells without any detectable side effects (Figure 17) [118].

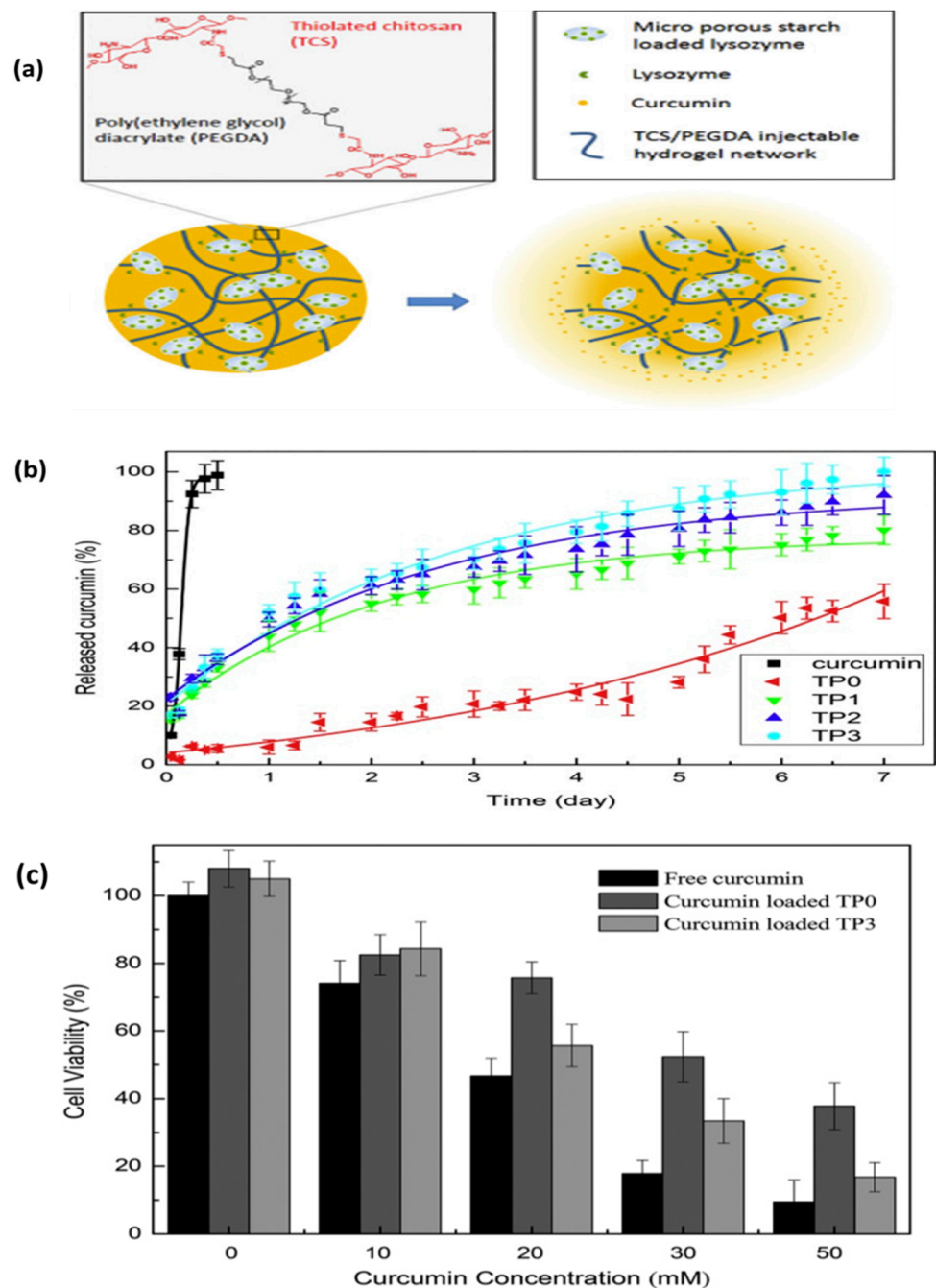


Figure 17. Cont.

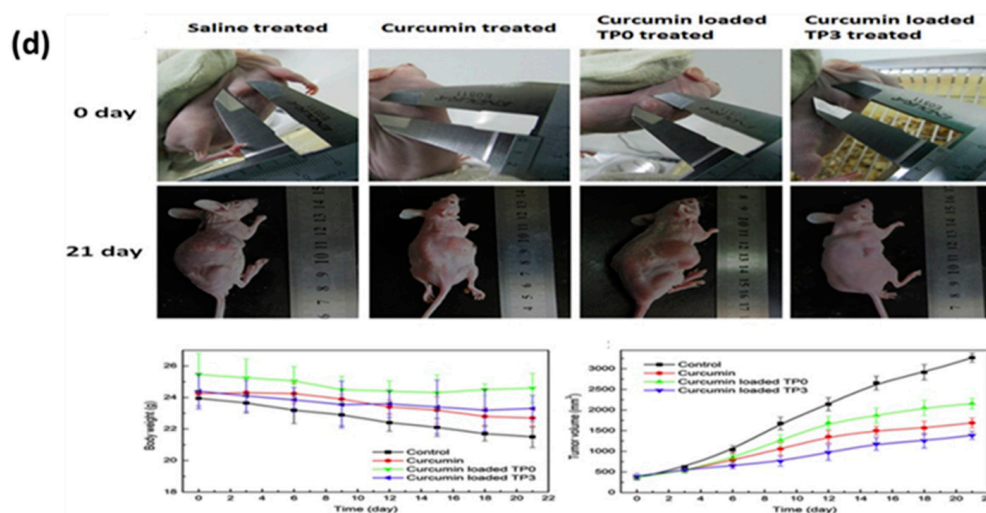


Figure 17. Scheme of preparation of injectable hydrogel by Michael addition crosslinking between thiolated chitosan and poly(ethylene glycol) diacrylate (TCS/PEGDA) for localized intratumoral delivery of curcumin (a); curcumin release behavior from TCS/PEGDA injectable hydrogel in PBS buffer at 37 °C with shaking (100 rpm) (b); HepG2 cells viability determined using MTT assay when incubated with free curcumin, and curcumin loaded TCS/PEGDA injectable hydrogels with (TP3) or without lysozyme, (TPO) respectively. Values are normalized to controls (cells without exposure to curcumin or hydrogels). (c); H&E staining of tumor, heart, liver, lung, and kidney tissue sections from tumor-bearing nude mice (scale bar: 50 μm) (d) and Histological analysis by hematoxylin and eosin staining of tumor, heart, liver, lung and kidney tissue from tumor-bearing nude mice (scale bar: 50 μm) (adapted with permission from Piao Ning et al., 2022).

4.1.1. Delivery of Antibiotic

The Schiff base crosslinking between the antibacterial *N*-(2-hydroxypropyl)-3-trimethylammonium chitosan chloride (HTCC) and polydextran aldehyde (PDA) offered dual-function, a pH-sensitive injectable hydrogel that was used for the local delivery of vancomycin. Interestingly, the hydrogels with higher vancomycin content extended the drug release up to 40 days at pH 7.2, reflecting the matrix's ability to control the release of vancomycin due to the reversible imine bonds formed between vancomycin and aldehyde groups along the dextran chains. The ability of the vancomycin-loaded gels to reduce the count of methicillin-resistant *staphylococcus aureus* (MARSA) upon subcutaneous implantation in mice. When MARSA were injected directly onto the same site where the gel was implanted or at \sim 1.5–2.0 cm distance, the gel showed (a 99.9999% reduction in MARSA count) compared to the nontreated tissue sample. Besides, the histopathology examination revealed that the group treated with vancomycin-loaded hydrogels had a slight inflammatory response at the infected skin site and the tissues surrounding the infected site compared to the control group (untreated hydrogel group), which suffered severe inflammatory responses. Interestingly, the active formulations that contain (PDA 2.5 wt%, HTCC 2.0% with 0.3 wt% vancomycin) showed no in vitro or in vivo hemolytic effect (Figure 18) [119].

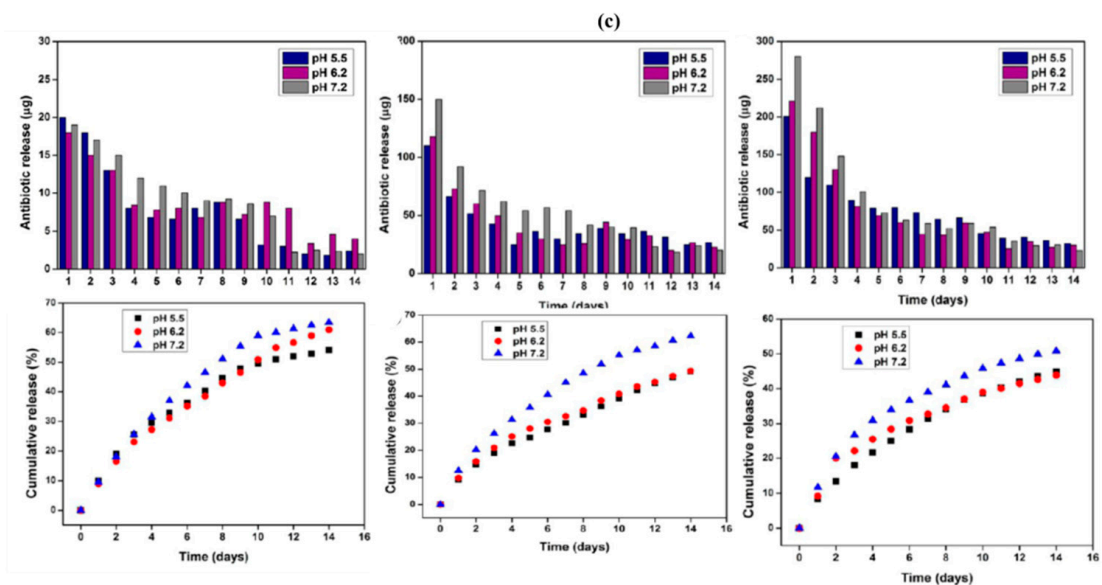
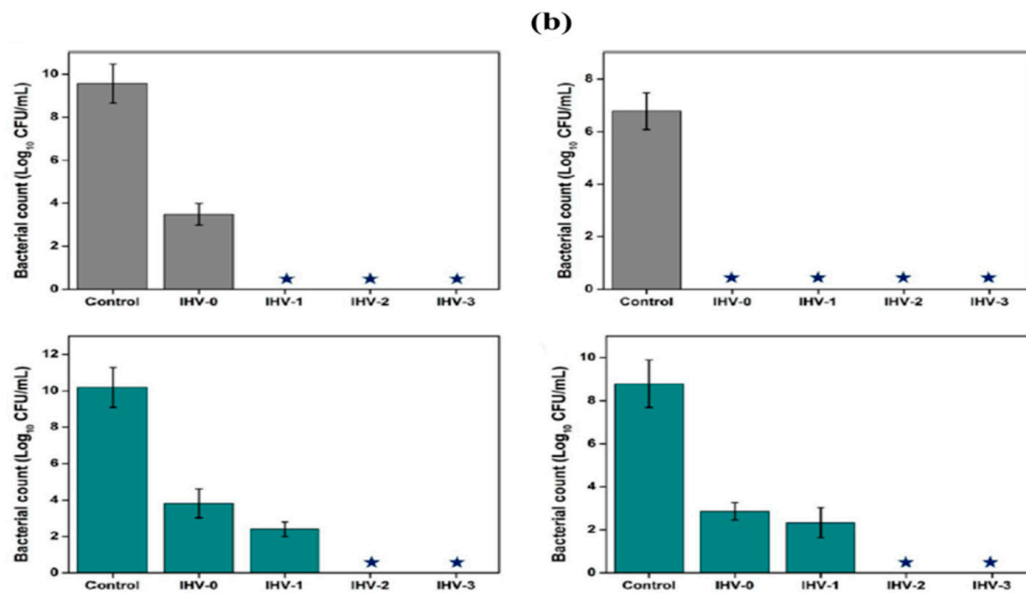
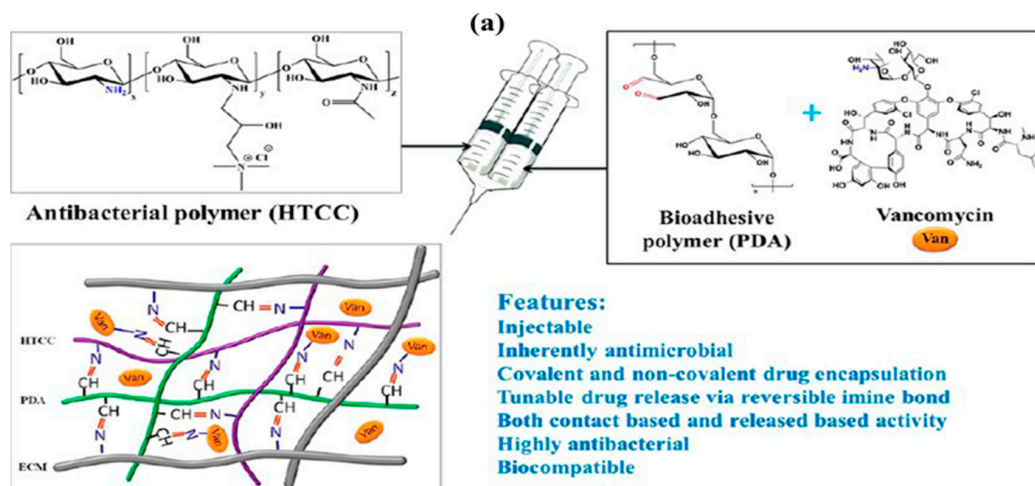


Figure 18. Cont.

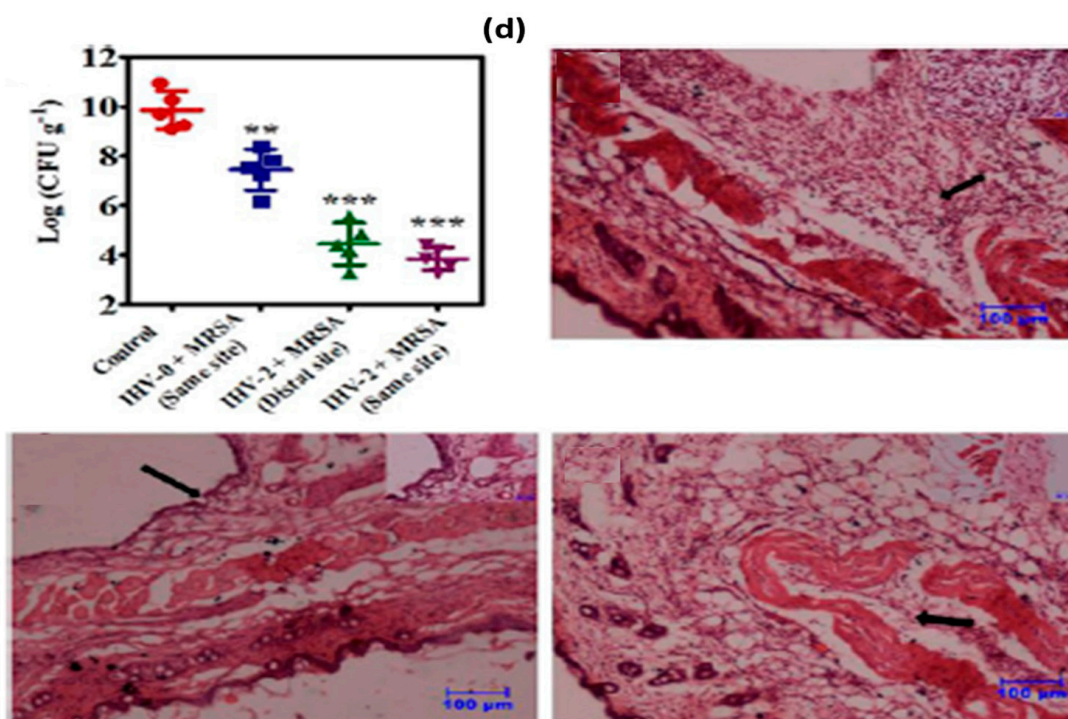


Figure 18. Schematic representation of the antibiotic loaded hydrogels (a); antibacterial activity of the hydrogels. Bacterial count after 6 h when 150 μ L of the pathogen (b); antibiotic release from the vancomycin-containing hydrogels (c); in vivo activity of the hydrogels. Evaluation of antibacterial activity upon injection of MRSA subcutaneously in mice (d) (*, ** and *** denotes to significant error) (adapted with permission from Hoque et al., 2018).

4.1.2. Protein and Growth Factors Delivery

Several studies have reported using smart hydrogels [103–105], particularly PSIHs for the immobilization of therapeutic proteins and growth factors [120–122]. Recently, X. Ma and his research group [123] reported the preparation of hydrazone-based IHs by coupling hydrazide-modified poly (γ -glutamic acid) (γ -PGA-ADH) aldehyde with aldehyde hyaluronic acid (HA-CHO). The hydrogels were used as delivery platforms for bovine serum albumin (BSA). Meanwhile, the self-crosslinking between aldehyde-hyaluronic acid with 3',3'-dithiobis (propanoic dihydrazide) conjugated hyaluronic, afforded a pH dual-responsive IH. Furthermore, the acyl hydrazone and disulfide linkages enabled the hydrogel's acid-switchable, shape-recovery, and self-healing abilities, and controlling the release of BSA encapsulated in this hydrogel was accomplished by either the change in the pH- or glutathione-mediated intracellular reduction for the disulfide bonds [124]. IHs for the encapsulation of growth factors proved efficient in many preclinical and clinical studies due to their ability to protect proteins against enzymatic degradation [21,120,125,126]. For example, the delivery of growth factors, including the vascular endothelial growth factor (VEGF) and recombinant bone morphogenetic protein 2 (BMP-2), by IHs, have been investigated by Divband et al. [127]. The hydrogels were prepared via the electrostatic interaction between cationic biguanidiny chitosan and anionic carboxymethyl cellulose. The tuned release profile of the growth factors from the hydrogel was consistent with the rate of human bone growth. Additionally, the Western blot and qRT-PCR assays indicated that BMP-2/VEGF-containing hydrogel potently induced the osteogenic differentiation of dental pulp stem cells, evidenced by the increased expression of ALP, collagen 1, and osteocalcin genes [127] as shown in Figure 19.

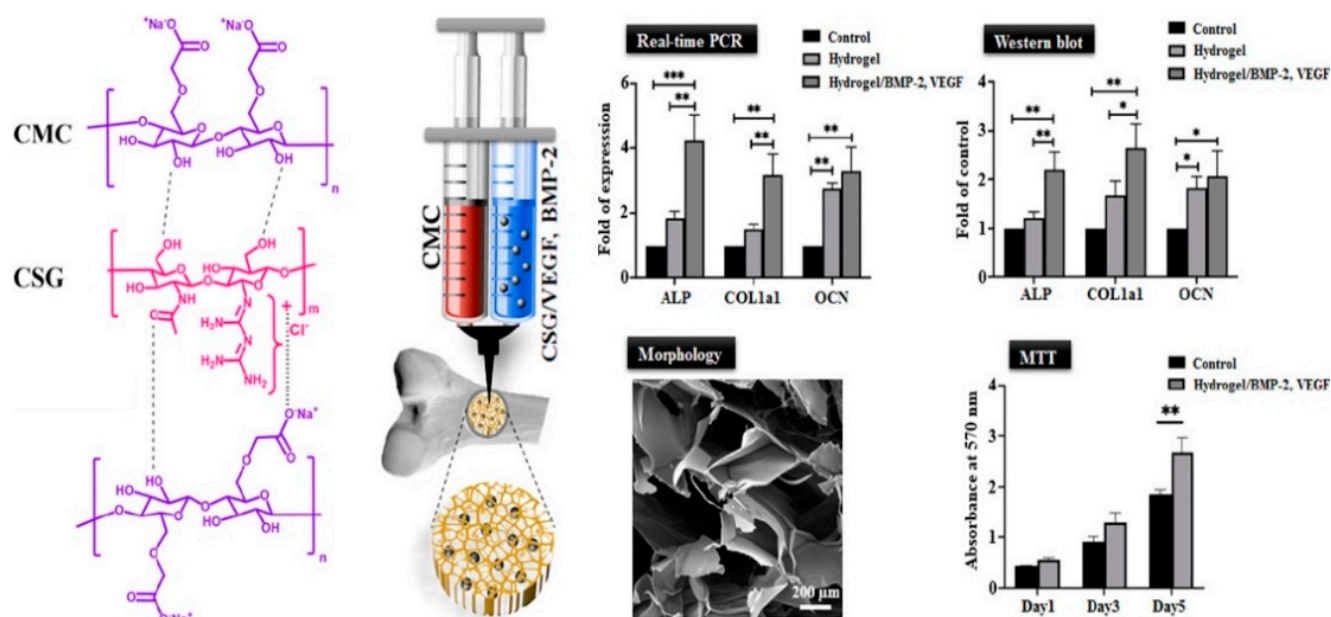


Figure 19. Synthesis of cationic biguanidinyl chitosan and anionic carboxymethylcellulose and its use in encapsulation of endothelial growth factor (VEGF) and recombinant bone morphogenetic protein 2 (rBMP-2) (*, ** and *** denotes to significant error) (adapted with permission from Divband et al., 2021).

4.1.3. Encapsulation of Cells

There have been an increasing number of reports that detail the use of IHs as unique intelligent materials for the encapsulation of cell therapeutics [128–130]. For example, the IHs developed by a physico-chemical interaction between Fe^{3+} and an alginate/gelatin mixture were evaluated for their capability to encapsulate murine bone calvaria pre-osteoblast (MC3T3-E1) cells and support their survival, proliferation, and osteogenic differentiation. The study revealed that cells' proliferation ability was similar to that of cells cultured on the standard tissue culture polystyrene (TCPS) dish. Likewise, the expression of the runt-related transcription factor-2 (RUNX2) gene, alkaline phosphatase (ALP) activity, and calcium precipitation rate were significantly higher for the cells engulfed in the hydrogels rather than the cells cultured in the TCPS dish [131]. Meanwhile, Miller and his research group developed a fibrous hydrogel following the advanced host-guest immobilization strategy. Hyaluronic acid (HA) was decorated with adamantane (guest) and interacted with HA modified with methacrylates and 6-(6-aminohexyl)amino-6-deoxy- β -cyclodextrin (host). Moreover, the presence of methacrylate moieties on HA enabled photo crosslinking for the hydrogel. Further electrospinning of HA produced nanofiber hydrogels with robust mechanical integrity, good shear-thinning behavior, rapid self-healing, and cyto-compatibility. The hydrogels strongly supported the viability of human mesenchymal stromal cells (hMSCs) after 7 days of culture (>85%) compared to the nonfibrous hydrogel (Figure 20) [132].

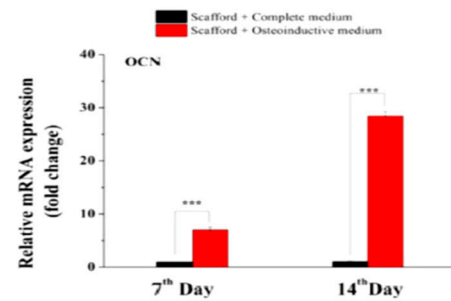
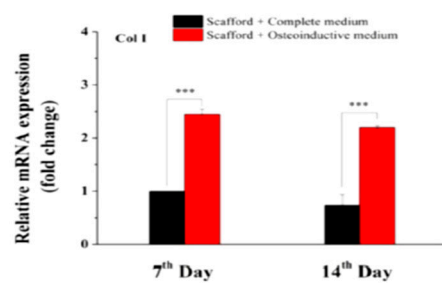
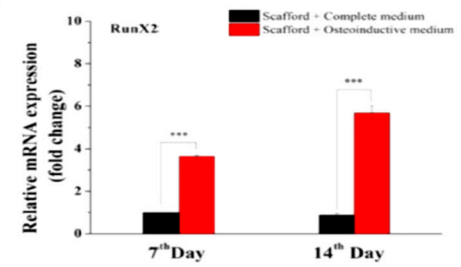
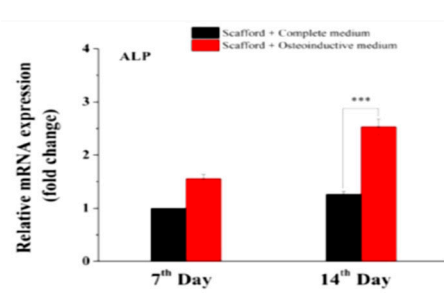
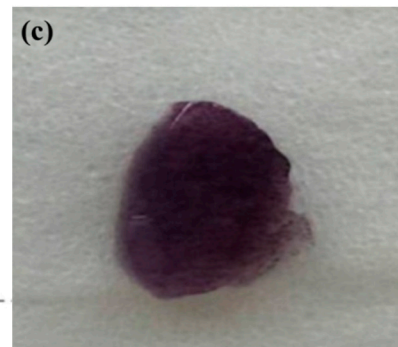
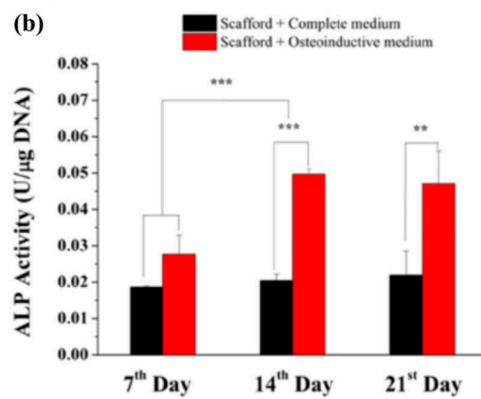
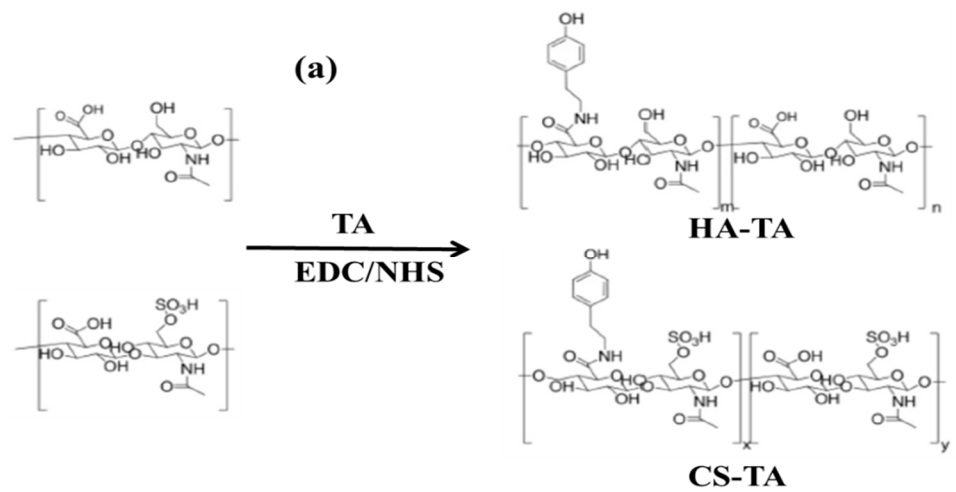


Figure 20. Cont.

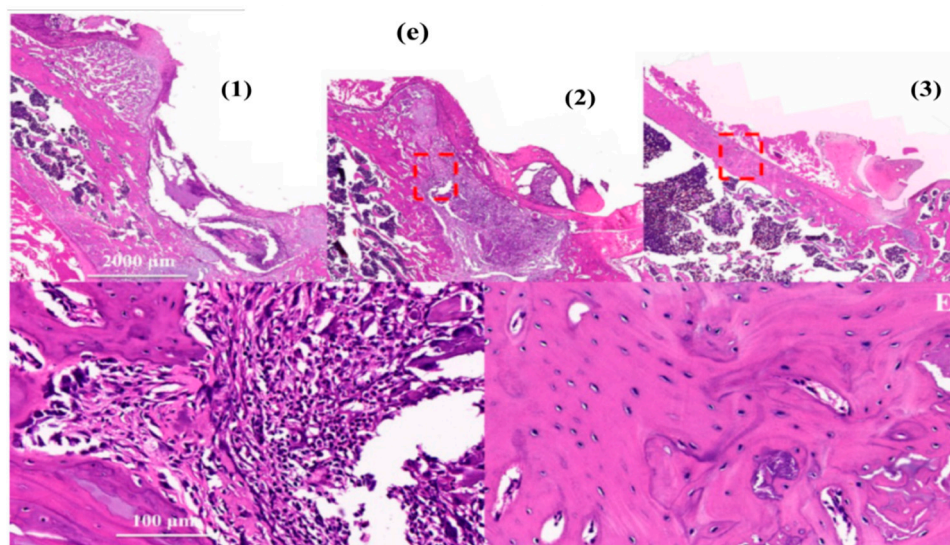


Figure 20. The synthesis route of BMSCs-laden injectable hydrogel (a), MSCs osteogenic differentiation within HA-CS hydrogels: The ALP activity of different groups (b), and the ALP staining (c); real-time PCR analysis: ALP, Col I, RunX2, and OCN expressions by BMSCs in the hydrogel after (d); incubation for 7 and 14 days; H&E staining of bone defect samples of different groups (e). Control group (1), control group at fourth week (2), the BMSCs-laden hydrogel encapsulated with BMP2 group at 4th week (3) (** and *** denotes to significant error) (adapted with permission from Miller et al., 2021).

4.2. Regenerative Medicine

4.2.1. Tissue Regeneration

Multi-featured IHs, with their porosity and viscoelasticity, adhesion, and self-healing properties, mimic the extracellular matrix [133]. IHs can regulate cell functions while permitting the diffusion of nutrients, metabolites, and growth factors [134]. According to Wang et al. [135], the IHs nanocomposite was prepared by coupling dialdehyde carboxymethyl dextran with dopamine via the Schiff base. Nano-hydroxyapatite/poly(L-glutamic acid) was loaded into the hydrogel and the resulting nanocomposite hydrogel successfully healed the rat cranial bone defect. Introducing bisphosphonate ligands (BPL) and nano-hydroxyapatite (nHA) effectively promoted the viability, proliferation, migration, and osteogenesis differentiation of MC3T3-E1 cells. The polypeptide poly(L-glutamic acid) (PLGA) was used to mimic collagen. At the same time, the presence of catechol motifs, BPL, and aldehyde groups endowed the adhesion and angiogenic capabilities of the hydrogel.

4.2.2. Wound Healing

Wound healing films with rapid anticoagulant, antimicrobial, and healing abilities are promising directions for curing serious cutaneous defects, especially in diabetic people and those with weak immune responses [136–138]. IHs capable of in situ gelation under physiological conditions have attracted intense research interest. The preference for IHs as emerging materials for wound healing is attributed to their ability to maintain a moist environment surrounding the wound interface, absorb the exudate, inhibit microbial infections, and allow the oxygen permeation to the covered tissue while cooling the surface of the injured area [139–141]. In this context, PSIHs have been extensively investigated for the fabrication of wound dressing films due to their biocompatibility, biodegradability, non-immunogenicity, and diversity in their physical properties and chemical structure [142–144].

Wang et al. [145] reported the development of dual-crosslinked multifeatured hydrogel as a wound dressing. Dialdehyde chitosan underwent self-crosslinking via Schiff base, forming the first hydrogel layer, and then phytic acid was crosslinked with the first layer via hydrogen bindings, affording a dual crosslinked tunable IHs. The resulting hydrogel

possessed inherent adhesion, self-healing, and antibacterial, good self-healing, and biocompatibility properties. These intrinsic properties endorse the two-layer hydrogel as an excellent candidate for biological applications, especially for wound dressings. Similarly, an injectable, antioxidant, conductive, self-healing, and antibacterial wound dressing hydrogel was fabricated by Schiff base coupling between quaternized chitosan-g-polyaniline (QCSP) and benzaldehyde functionalized poly(ethylene glycol)-co-poly(glycerol sebacate) (PEGS-FA). When the crosslinking ratio reached (1.5 wt%) the hydrogel (QCSP-PEGS-FA) showed excellent *in vivo* coagulation (Figure 21) and significantly enhanced the wound healing process *in vivo* abilities in full-thickness skin defect model compared to the QCS without polyaniline/PEGS-FA hydrogel and commercial dressing (Tegaderm™ film). The biochemical analysis demonstrated the ability of the hydrogel to cure the injury through upregulating the gene expression for growth factors, namely, VEGF, EGF, and TGF- β and promoting granulation tissue thickness and collagen deposition [139].

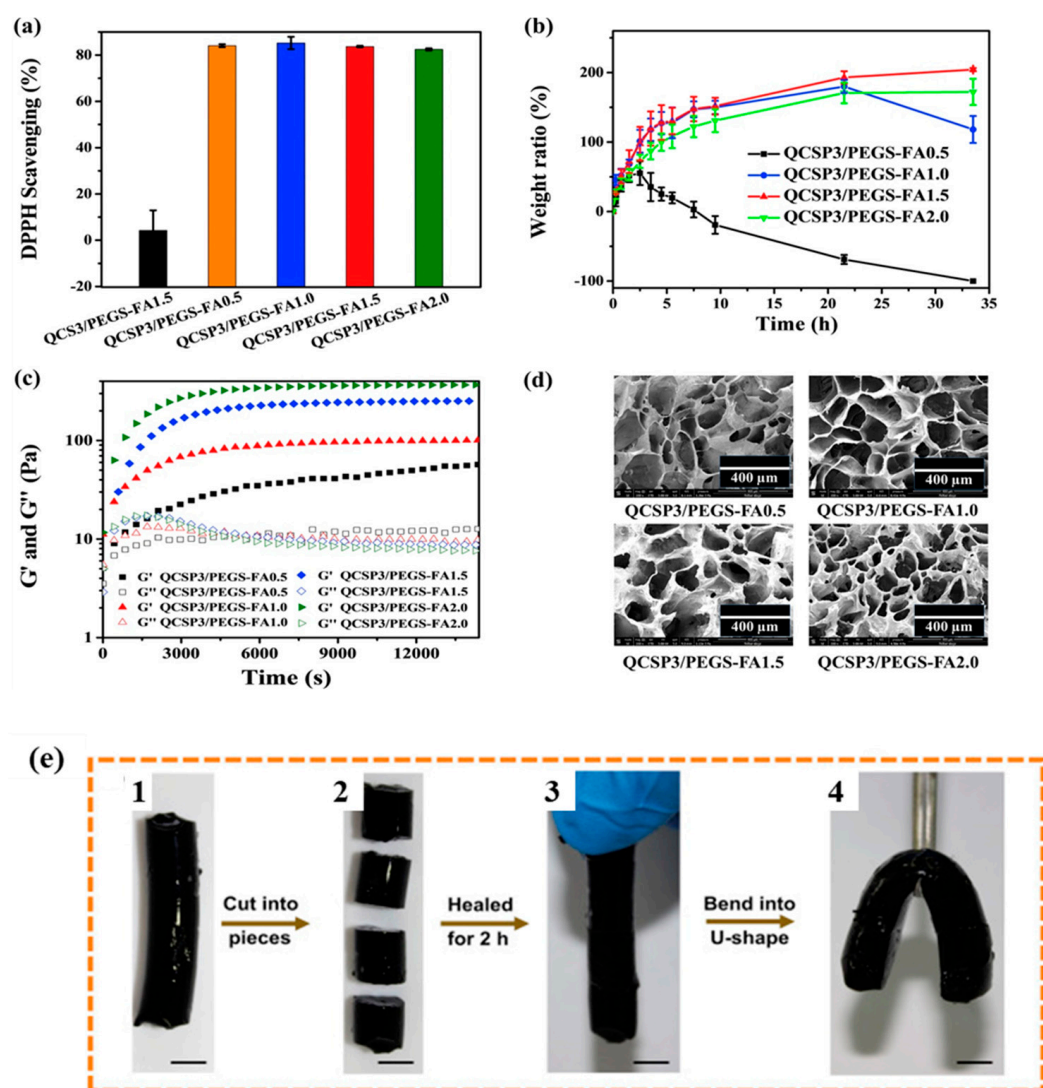


Figure 21. Cont.

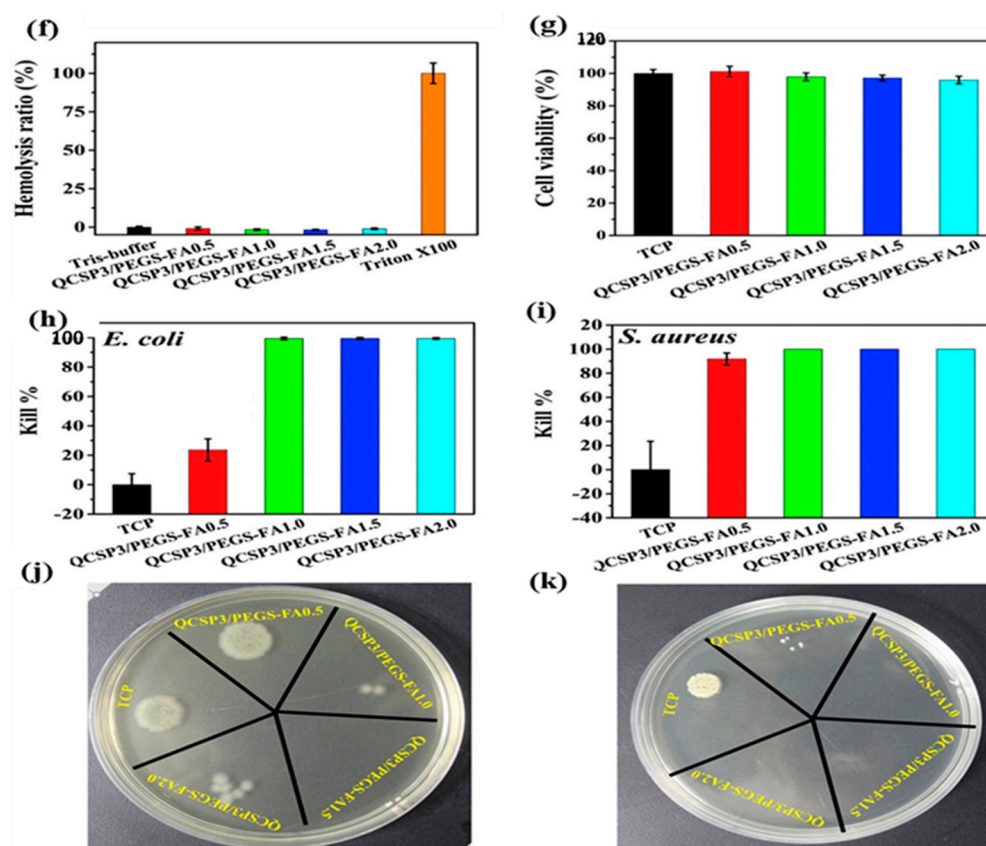


Figure 21. DPPH scavenging percentage by the hydrogels (a); weight ratio of the hydrogel in PBS at 37 °C for different time periods (b), rheological performance of the hydrogels (c), morphologies structure (d), self-healing property (e), anti-hemolytic ability (f), histocompatibility (g), antimicrobial activity (h–k) (adapted with permission from Zhao et al., 2017).

Additionally, hyaluronic acid modified with 2-amino phenylboronic acid immediately gelled upon mixing with different amounts of tannic acid (TA) and afforded multifunctional dynamic hydrogels with features that promise their use as wound dressings for chronic wound healing. TA served as a reductant for the silver ion, hydrogel precursor, and adhesive agent. The hydrogel loaded with silver nanoparticles showed pH response and reactive oxygen species scavenging capacity, cytocompatibility with potent and broad-spectrum antimicrobial activity [144]. Yang et al. [146], reported the preparation of dynamic IHs using oxidized hyaluronic acid (HA-CHO) which crosslinked with the free thiol groups in cysteine-grafted poly(γ -glutamic acid). The coupling is processed via thiol-aldehyde addition (TAA) under physiological conditions. The hydrogel revealed good self-healing capability, adjustable viscoelasticity in vitro and in vivo degradation properties, and antioxidant activity. The hydrogel significantly enhanced in vitro and in vivo the process of wound healing in a full-thickness skin defect model by facilitating angiogenesis and collagen deposition compared to the commercial dressing (Tegaderm™).

Recent studies are focusing on the innovation of wound dressing for healing chronic diabetic wounds. In this regard, K. Zhang et al. constructed a bioactive hydrogel in the “Pull–Push” approach for treating bacteria-infected diabetic wounds. The hydrogel was engineered via the Schiff base reaction between the cationic polymer polyethylenimine (PEI), tobramycin (Tob), and oxidized carboxymethyl cellulose (OCMC). Consequently, this multifunctional hydrogel (injectability, self-healing, and biocompatibility, pH sensitivity) exhibited remarkable capability of trapping the negatively charged biomolecules such as cell-free DNA, lipopolysaccharides, and tumor necrosis factor- α . This scavenging ability ameliorated the hydrogel anti-inflammation effects, sustained the release of Tob loaded into

the hydrogel, and greatly accelerated the rate of wound closure in *Pseudomonas aeruginosa*-infected diabetic wounds [147].

4.3. Biosensors and Implantable Biomedical Devices

High-performance strain sensors have gained enormous importance for their applications in wearable devices, artificial intelligence, soft robots, and implantable biomedical devices. However, the difficulties of high sensitivity, excellent mechanical properties, strong adhesion, and self-healing abilities, and simplicity of construction [148–152]. The integration of electric conductive polymers or nanofillers, such as polypyrrene (PPy), polythiophene [55], polyaniline (PANI), carbon nanotubes, and metallic nanoparticles into the IHs, contributed to endowing the hydrogel with the electric conductivity permitting their use in motion and strain sensors [153–156].

A novel dual ionic, conductive, self-healing IHs was produced by ion complexations and hydrogen bonding between Fe^{3+} , dialdehyde cellulose nanofibers (DACNFs), and the carboxyl groups of acrylic acid (AA). When the hydrogels were configured for a wearable test, some formulations demonstrated high stretching sensitivity with a gauge factor of 13.82 at a strain within 1.6%. The gauge factor (GF) decreased with the incremental strain within 20%. While the GF was 0.696 between 20 and 300% strain, when it was 0.837 between 300 and 500% [157]. Additionally, Pan et al. [158] developed mussel-inspired injectable nanocomposite hydrogels by the dispersion of proanthocyanins-coated cellulose nanofibrils (CNF) into a guar gum (GG) and glycerol solution to prepare (PC-CNF-GG-glycerol). This hydrogel exhibits great adhesion (7.9 KPa), UV-blocking ability (82%), and ion conductivity. The strain sensor assembled from the hydrogel exhibited low-weight detection ability (200 mg) and fast response speed (33 ms). It can also be used for preparing wearable, portable, and editable electrodes. The new electrode can accurately detect human electrophysiological signals. In another attempt, the multifeatured chitosan-based hydrogel was fabricated via a Schiff base linkage and hydrogen bonds. The hydrogel demonstrated desirable injectability, self-healing, and conductivity with pH sensitivity, and intrinsic broad-spectrum antibacterial properties. Moreover, it accelerated the in vivo healing for a full-thickness skin-wound model to confirm its outstanding effect on wound healing. Moreover, the conductive chitosan-based hydrogel can be used as epidermal sensors that distinguish various human activities in real-time during the time of wound healing [159]. In a different approach, Zhao et al. engineered motion sensors successfully from IHs packed by embedding silver nanowires into methacrylate alginate film, which underwent in situ gelations via photopolymerization under green light irradiation [160]. The resulting sensors possessed characteristic adhesion ability on the skin and organs conformal adhesion (0.24–1.53 kPa), and precise sensitivity for human motions and electrophysiological signal (GF = 1.63 at a strain range of 0–100%). Moreover, the sensors showed good transparency (~85% transmittance) and reusability, contributing to reducing electronic waste and environmental burden (Figure 22).

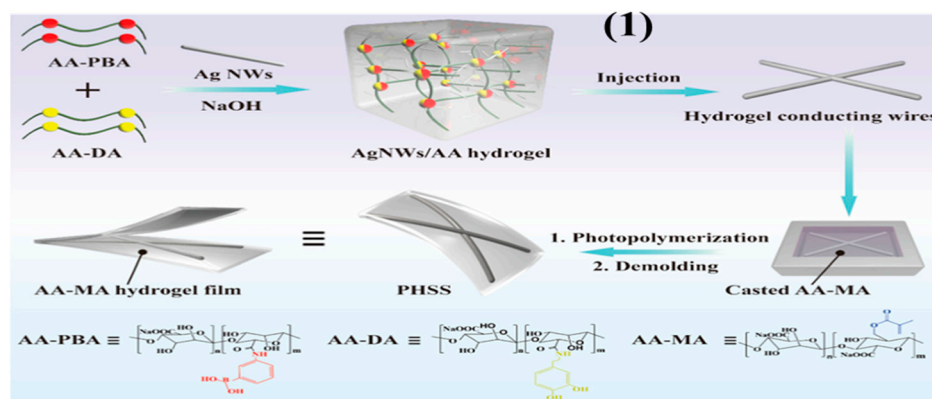


Figure 22. Cont.

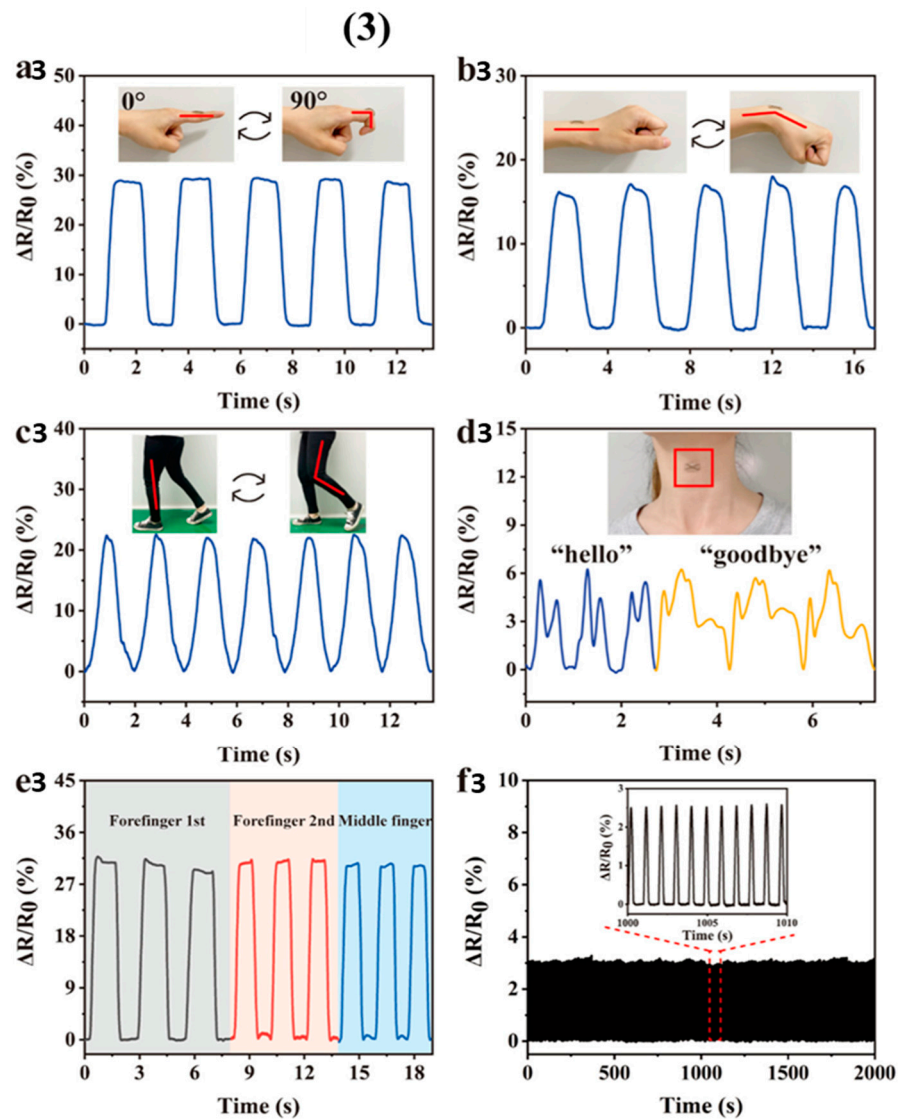
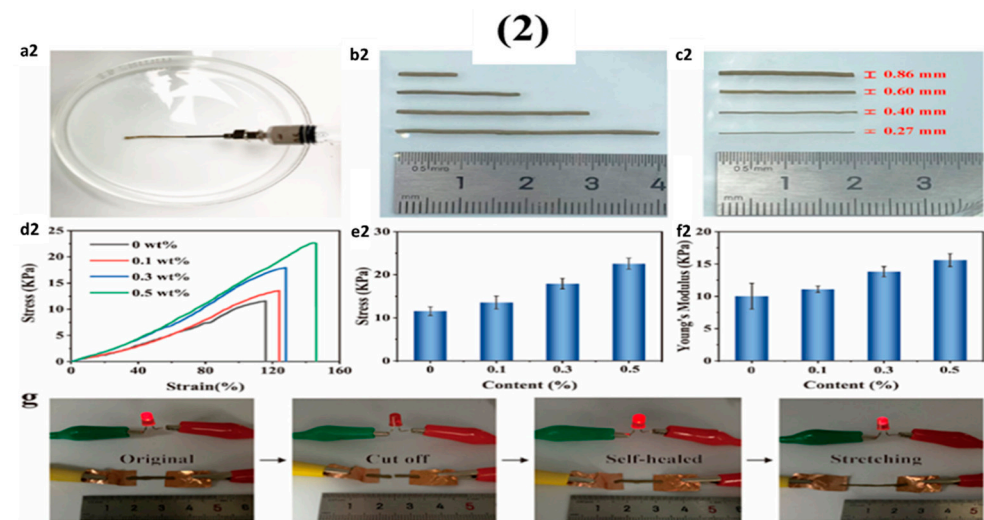


Figure 22. Fabrication procedures and schematic structures of PHSSs (1); mechanical and conductive properties of injected Ag NWs/AA hydrogel wires (2); application of the PHSS as strain and motion sensors (3) (adapted with permission from Zhao et al., 2022).

5. Status and Perspectives

Injectable hydrogels (IHs) have emerged as a smart class of biomaterials and revealed significant advantages when employed in the pharmaceutical field, achieving site selectivity and controlled release for the therapeutic agent in response to the change in the physical stimuli (pH, temperature, or enzyme concentration). On the other hand, the robust mechanical properties and shear-thinning of IHs proved superior performance when used as scaffolds for regenerative medicine.

Most IHs can be prepared through physical or chemical crosslinking of the precursor solutions when subjected to external stimuli. In this regard, the gelation rate and the degree of injectability are the key factors that govern the suitability of the hydrogels for actual applications. The injection rate of IHs is mainly affected by the viscosity of the hydrogel-forming precursors. Highly viscous solutions will block the injection needle, while very low viscous solutions will influence the gelation time. Multistimuli-sensitive IHs must be developed to solve clogging issues during the injection, including the combination of pH and temperature-sensitive copolymers.

The formation of IHs with the desired phase transition rate and combined with its features the good self-adhesion and self-healing abilities are beneficial for tissue regeneration.

Electric conductivity, flexibility, and stretchability of IHs are the keywords for their application as strain and motion sensors. While biocompatibility is a critical concern since the polymers used to assemble the hydrogels and the IHs resulting from the polymers' crosslinking must not be cytotoxic or cause any devastating actions to the tissues or whole body when injected *in vivo*. In this regard, researchers worldwide focus on using polysaccharides to substitute petroleum-derived polymers partially or entirely. Moreover, the biodegradation rate of IHs must be tuned according to the application requirements. For instance, successful IHs used as scaffolds for tissue regeneration, wound healing, or drug delivery platforms should exhibit a biodegradation rate that is proportional to the growth and proliferation of the new cells. While IHs employed in drug delivery, their biodegradability and clearance should not begin until they deliver the cargo to the target tissue. Selecting a suitable polysaccharide polymer and applying two or more different crosslinking mechanisms to ensure rapid responsiveness and hydrogel stability are highly recommended, particularly for site-selective and controlled release of drugs from the IHs.

There are problems with *in vivo* IHs, should the stability and ability to encapsulate the active therapeutics or cells should be taken into consideration. Among the proposed solution to overcome the hydrogel stability is the design of dual or multi-crosslinked PSIHs that can withstand the microenvironmental changes while releasing their payload in a controlled manner.

Although the biocompatibility, structure diversity, and low cost of polysaccharides, they suffer the problem of poor mechanical properties compared to synthetic polymers. Therefore, the development of advanced hybrid hydrogels that combine in their composition both the polysaccharides and biocompatible synthetic polymers, e.g., polyurethanes, polyester, and peptides, greatly improved the mechanical properties of the hydrogels while retaining their biocompatibility feature.

Much progress has been made in applying IHs to treating diseases, repairing, and regenerating tissues, sustained release of nutrients, and so on. However, some critical problems still exist and restrict their applications. For instance, most of the physically crosslinked IHs are temperature-responsive. Still, increasing the temperature above room temperature during the subcutaneous injection might accelerate the gelation rate before the infusion. Additionally, the interaction between the payload and the hydrogels, such as electrostatic interactions, hydrogen bonding, hydrophobic chemical bonding, etc., must be considered when designing the hydrogel to adjust the release kinetics.

Most biocompatibility studies focus on the evaluation of hydrogel toxicity. However, toxicity studies on the fate of hydrogel biodistribution, its biodegradation products, and their toxicity profiles must also be considered to ensure the long-term safety of the hydrogel before and after biodegradation.

Future studies and research should address the problems associated with using IHs. This includes the fabrication techniques, the solvents used to dissolve the polymers, the mechanical performance, the response to external stimuli, the stability in the bloodstream, the production cost, and scaling up to credit IHs the qualifications needed for their actual applications. Environmental concerns must be regarded during the fabrication of IHs. Finally, progress in the field of material science and nanotechnology and the increasing need for smart materials can effectively contribute to creating multifeatured, multifunctional IHs to meet the growing demands. In addition, the development of IHs with more advanced properties should be further explored to provide more options for various applications.

6. Conclusions

Injectable hydrogels (IHs) are an important class of materials in light of the drive in the clinic toward minimally invasive procedures. Developments in polymer science provide an opportunity for more sophisticated IHs with various and useful properties. As is demonstrated in this review, exciting research is underway for many different systems. Understanding the chemical mechanisms of different crosslinking mechanisms is of great significance for designing smart injectable hydrogels for biomedical applications. Hydrogels with proper pH responsiveness, good biocompatibility, and injectability are required for selective localization sites and to control the release of drugs into the target. Meanwhile, developing IHs with self-healing properties, bioprinting, adhesives, and a tunable biodegradation rate allowed their application in wound healing and tissue regeneration. Several research groups innovated smart injectable systems hydrogels by incorporating several elements and applying dual crosslinking mechanisms to ensure robust mechanical properties and superior sensitivity to external stimuli.

Author Contributions: S.K. and N.S.E.-S. conducted and completed writing, addressing, reformatting, proofreading, and editing the review manuscript. All authors have read and agreed to the published version of the manuscript.

Funding: This research received no external funding.

Data Availability Statement: Not applicable.

Acknowledgments: Authors are thankful for the technical support from National Research Centre, Egypt.

Conflicts of Interest: The authors declare no conflict of interest.

References

1. Liu, Z.; Jiao, Y.; Wang, Y.; Zhou, C.; Zhang, Z. Polysaccharides-based nanoparticles as drug delivery systems. *Adv. Drug Deliv. Rev.* **2008**, *60*, 1650–1662. [[CrossRef](#)] [[PubMed](#)]
2. Mohammed, A.S.A.; Naveed, M.; Jost, N. Polysaccharides; classification, chemical properties, and future perspective applications in fields of pharmacology and biological medicine (A review of current applications and upcoming potentialities). *J. Polym. Environ.* **2021**, *29*, 2359–2371. [[CrossRef](#)]
3. El-Sayed, N.S.; Sharma, M.; Aliabadi, H.M.; El-Meligy, M.G.; El-Zaity, A.K.; Nageib, Z.A.; Tiwari, R.K. Synthesis, characterization, and in vitro cytotoxicity of fatty acyl-CGKRK-chitosan oligosaccharides conjugates for siRNA delivery. *Int. J. Biol. Macromol.* **2018**, *112*, 694–702. [[CrossRef](#)]
4. El-Sayed, N.S.; Sajid, M.I.; Parang, K.; Tiwari, R.K. Synthesis, characterization, and cytotoxicity evaluation of dextran-myristoyl-ECGKRK peptide conjugate. *Int. J. Biol. Macromol.* **2021**, *191*, 1204–1211. [[CrossRef](#)]
5. El-Sayed, N.S.; El-Sakhawy, M.; Hesemann, P.; Brun, N.; Kamel, S. Rational design of novel water-soluble ampholytic cellulose derivatives. *Int. J. Biol. Macromol.* **2018**, *114*, 363–372. [[CrossRef](#)]
6. El-Sayed, N.S.; Salama, A.; Guarino, V. Coupling of 3-Aminopropyl Sulfonic Acid to Cellulose Nanofibers for Efficient Removal of Cationic Dyes. *Materials* **2022**, *15*, 6964. [[CrossRef](#)]
7. Yu, Y.; Shen, M.; Song, Q.; Xie, J. Biological activities and pharmaceutical applications of polysaccharide from natural resources: A review. *Carbohydr. Polym.* **2018**, *183*, 91–101. [[CrossRef](#)] [[PubMed](#)]
8. El-Sayed, N.S.; El-Sakhawy, M.; Brun, N.; Hesemann, P.; Kamel, S. New approach for immobilization of 3-aminopropyltrimethoxysilane and TiO₂ nanoparticles into cellulose for BJ1 skin cells proliferation. *Carbohydr. Polym.* **2018**, *199*, 193–204. [[CrossRef](#)] [[PubMed](#)]

9. Yadav, H.; Karthikeyan, C. *Natural Polysaccharides: Structural Features and Properties. Polysaccharide Carriers for Drug Delivery*; Elsevier: Amsterdam, The Netherlands, 2019; pp. 1–17.
10. Turkey, G.; Moussa, M.A.; Hasanin, M.; El-Sayed, N.S.; Kamel, S. Carboxymethyl cellulose-based hydrogel: Dielectric study, antimicrobial activity and biocompatibility. *Arab. J. Sci. Eng.* **2021**, *46*, 17–30. [[CrossRef](#)]
11. EL-Sayed, N.S.; El-Ziaty, A.; El-Meligy, M.G.; Nagieb, Z.A. Syntheses of New Antimicrobial Cellulose Materials Based 2-((2-aminoethyl) amino)-4-aryl-6-indolylnicotinonitriles. *Egypt. J. Chem.* **2017**, *60*, 465–477.
12. El-Sayed, N.S.; Moussa, M.A.; Kamel, S.; Turkey, G. Development of electrical conducting nanocomposite based on carboxymethyl cellulose hydrogel/silver nanoparticles@ polypyrrole. *Synth. Met.* **2019**, *250*, 104–114. [[CrossRef](#)]
13. Mellati, A.; Akhtari, J. Injectable hydrogels: A review of injectability mechanisms and biomedical applications. *Res. Mol. Med. (RMM)* **2019**, *250*, 104–114. [[CrossRef](#)]
14. El-Sayed, N.S.; Awad, H.; El-Sayed, G.M.; Nagieb, Z.A.; Kamel, S. Synthesis and characterization of biocompatible hydrogel based on hydroxyethyl cellulose-g-poly (hydroxyethyl methacrylate). *Polym. Bull.* **2020**, *77*, 6333–6347. [[CrossRef](#)]
15. Ahmed, E.M. Hydrogel: Preparation, characterization, and applications: A review. *J. Adv. Res.* **2015**, *6*, 105–121. [[CrossRef](#)] [[PubMed](#)]
16. El-Sayed, N.S.; Al Kiey, S.A.; Darwish, A.; Turkey, G.; Kamel, S. High performance hydrogel electrodes based on sodium alginate-g-poly (AM-c o-ECA-co-AMPS for supercapacitor application. *Int. J. Biol. Macromol.* **2022**, *218*, 420–430. [[CrossRef](#)] [[PubMed](#)]
17. Reddy, N.; Reddy, R.; Jiang, Q. Crosslinking biopolymers for biomedical applications. *Trends Biotechnol.* **2015**, *33*, 362–369. [[CrossRef](#)]
18. Chai, Q.; Jiao, Y.; Yu, X. Hydrogels for biomedical applications: Their characteristics and the mechanisms behind them. *Gels* **2017**, *3*, 6. [[CrossRef](#)]
19. Bai, X.; Lü, S.; Liu, H.; Cao, Z.; Ning, P.; Wang, Z.; Gao, C.; Ni, B.; Ma, D.; Liu, M. Polysaccharides based injectable hydrogel compositing bio-glass for cranial bone repair. *Carbohydr. Polym.* **2017**, *175*, 557–564. [[CrossRef](#)]
20. Overstreet, D.J.; Dutta, D.; Stabenfeldt, S.E.; Vernon, B.L. Injectable hydrogels. *J. Polym. Sci. Part B Polym. Phys.* **2012**, *50*, 881–903. [[CrossRef](#)]
21. Mathew, A.P.; Uthaman, S.; Cho, K.-H.; Cho, C.-S.; Park, I.-K. Injectable hydrogels for delivering biotherapeutic molecules. *Int. J. Biol. Macromol.* **2018**, *110*, 17–29. [[CrossRef](#)]
22. Hennink, W.E.; van Nostrum, C.F. Novel crosslinking methods to design hydrogels. *Adv. Drug Deliv. Rev.* **2012**, *64*, 223–236. [[CrossRef](#)]
23. You, J.; Cao, J.; Zhao, Y.; Zhang, L.; Zhou, J.; Chen, Y. Improved mechanical properties and sustained release behavior of cationic cellulose nanocrystals reinforced cationic cellulose injectable hydrogels. *Biomacromolecules* **2016**, *17*, 2839–2848. [[CrossRef](#)] [[PubMed](#)]
24. Wang, K.; Nune, K.; Misra, R. The functional response of alginate-gelatin-nanocrystalline cellulose injectable hydrogels toward delivery of cells and bioactive molecules. *Acta Biomater.* **2016**, *36*, 143–151. [[CrossRef](#)] [[PubMed](#)]
25. Ghorbani, M.; Roshangar, L.; Rad, J.S. Development of reinforced chitosan/pectin scaffold by using the cellulose nanocrystals as nanofillers: An injectable hydrogel for tissue engineering. *Eur. Polym. J.* **2020**, *130*, 109697. [[CrossRef](#)]
26. Shen, Y.; Li, X.; Huang, Y.; Chang, G.; Cao, K.; Yang, J.; Zhang, R.; Sheng, X.; Ye, X. pH and redox dual stimuli-responsive injectable hydrogels based on carboxymethyl cellulose derivatives. *Macromol. Res.* **2016**, *24*, 602–608. [[CrossRef](#)]
27. Sultana, T.; Van Hai, H.; Abueva, C.; Kang, H.J.; Lee, S.-Y.; Lee, B.-T. TEMPO oxidized nano-cellulose containing thermo-responsive injectable hydrogel for post-surgical peritoneal tissue adhesion prevention. *Mater. Sci. Eng. C* **2019**, *102*, 12–21. [[CrossRef](#)]
28. Yang, J.-A.; Yeom, J.; Hwang, B.W.; Hoffman, A.S.; Hahn, S.K. In situ-forming injectable hydrogels for regenerative medicine. *Prog. Polym. Sci.* **2014**, *39*, 1973–1986. [[CrossRef](#)]
29. Wang, P.; Zhang, J.; Li, Y.; Wang, N.; Liu, W. A nucleoside responsive diaminotriazine-based hydrogen bonding strengthened hydrogel. *Mater. Lett.* **2015**, *142*, 71–74. [[CrossRef](#)]
30. Zheng, L.Y.; Shi, J.M.; Chi, Y.H. Tannic acid physically cross-linked responsive hydrogel. *Macromol. Chem. Phys.* **2018**, *219*, 1800234. [[CrossRef](#)]
31. Ma, M.; Zhong, Y.; Jiang, X. Thermosensitive and pH-responsive tannin-containing hydroxypropyl chitin hydrogel with long-lasting antibacterial activity for wound healing. *Carbohydr. Polym.* **2020**, *236*, 116096. [[CrossRef](#)]
32. Geng, H.; Dai, Q.; Sun, H.; Zhuang, L.; Song, A.; Caruso, F.; Hao, J.; Cui, J. Injectable and sprayable polyphenol-based hydrogels for controlling hemostasis. *ACS Appl. Bio Mater.* **2020**, *3*, 1258–1266. [[CrossRef](#)]
33. You, S.; Xiang, Y.; Qi, X.; Mao, R.; Cai, E.; Lan, Y.; Lu, H.; Shen, J.; Deng, H. Harnessing a biopolymer hydrogel reinforced by copper/tannic acid nanosheets for treating bacteria-infected diabetic wounds. *Mater. Today Adv.* **2022**, *15*, 100271. [[CrossRef](#)]
34. Liu, C.; Yang, L.; Qiao, L.; Liu, C.; Zhang, M.; Jian, X. An injectable and self-healing novel chitosan hydrogel with low adamantane substitution degree. *Polym. Int.* **2019**, *68*, 1102–1112. [[CrossRef](#)]
35. Debele, T.A.; Mekuria, S.L.; Tsai, H.-C. Polysaccharide based nanogels in the drug delivery system: Application as the carrier of pharmaceutical agents. *Mater. Sci. Eng. C* **2016**, *68*, 964–981. [[CrossRef](#)]
36. Leganés, J.; Sánchez-Migallón, A.; Merino, S.; Vázquez, E. Stimuli-responsive graphene-based hydrogel driven by disruption of triazine hydrophobic interactions. *Nanoscale* **2020**, *12*, 7072–7081. [[CrossRef](#)]

37. Rizzo, F.; Kehr, N.S. Recent advances in injectable hydrogels for controlled and local drug delivery. *Adv. Healthc. Mater.* **2021**, *10*, 2001341. [[CrossRef](#)]
38. Hsiao, M.-H.; Larsson, M.; Larsson, A.; Evenbratt, H.; Chen, Y.-Y.; Chen, Y.-Y.; Liu, D.M. Design and characterization of a novel amphiphilic chitosan nanocapsule-based thermo-gelling biogel with sustained in vivo release of the hydrophilic anti-epilepsy drug ethosuximide. *J. Control. Release* **2012**, *161*, 942–948. [[CrossRef](#)]
39. Lu, K.-Y.; Lin, Y.-C.; Lu, H.-T.; Ho, Y.-C.; Weng, S.-C.; Tsai, M.-L.; Mi, F.-L. A novel injectable in situ forming gel based on carboxymethyl hexanoyl chitosan/hyaluronic acid polymer blending for sustained release of berberine. *Carbohydr. Polym.* **2019**, *206*, 664–673. [[CrossRef](#)]
40. Geng, Z.; Ji, Y.; Yu, S.; Liu, Q.; Zhou, Z.; Guo, C.; Lu, D.; Pei, D. Preparation and characterization of a dual cross-linking injectable hydrogel based on sodium alginate and chitosan quaternary ammonium salt. *Carbohydr. Res.* **2021**, *507*, 108389. [[CrossRef](#)]
41. Pettinelli, N.; Rodriguez-Llamazares, S.; Bouza, R.; Barral, L.; Feijoo-Bandin, S.; Lago, F. Carrageenan-based physically crosslinked injectable hydrogel for wound healing and tissue repairing applications. *Int. J. Pharm.* **2020**, *589*, 119828. [[CrossRef](#)]
42. Chen, W.; Bu, Y.; Li, D.; Liu, C.; Chen, G.; Wan, X.; Li, N. High-strength, tough, and self-healing hydrogel based on carboxymethyl cellulose. *Cellulose* **2020**, *27*, 853–865. [[CrossRef](#)]
43. Mahdavinia, G.R.; Karimi, M.H.; Soltaniniya, M.; Massoumi, B. In vitro evaluation of sustained ciprofloxacin release from κ -carrageenan-crosslinked chitosan/hydroxyapatite hydrogel nanocomposites. *Int. J. Biol. Macromol.* **2019**, *126*, 443–453. [[CrossRef](#)]
44. Liu, G.; Yuan, Q.; Hollett, G.; Zhao, W.; Kang, Y.; Wu, J. Cyclodextrin-based host–guest supramolecular hydrogel and its application in biomedical fields. *Polym. Chem.* **2018**, *9*, 3436–3449. [[CrossRef](#)]
45. Ma, X.; Zhao, Y. Biomedical applications of supramolecular systems based on host–guest interactions. *Chem. Rev.* **2015**, *115*, 7794–7839. [[CrossRef](#)]
46. Dong, S.; Zheng, B.; Wang, F.; Huang, F. Supramolecular polymers constructed from macrocycle-based host–guest molecular recognition motifs. *Acc. Chem. Res.* **2014**, *47*, 1982–1994. [[CrossRef](#)]
47. Loh, X.J. Supramolecular host–guest polymeric materials for biomedical applications. *Mater. Horiz.* **2014**, *1*, 185–195. [[CrossRef](#)]
48. Almawash, S.; El Hamd, M.A.; Osman, S.K. Polymerized β -Cyclodextrin-Based Injectable Hydrogel for Sustained Release of 5-Fluorouracil/Methotrexate Mixture in Breast Cancer Management: In Vitro and In Vivo Analytical Validations. *Pharmaceutics* **2022**, *14*, 817. [[CrossRef](#)]
49. Hu, Q.-D.; Tang, G.-P.; Chu, P.K. Cyclodextrin-based host–guest supramolecular nanoparticles for delivery: From design to applications. *Acc. Chem. Res.* **2014**, *47*, 2017–2025. [[CrossRef](#)]
50. Okubo, M.; Iohara, D.; Anraku, M.; Higashi, T.; Uekama, K.; Hirayama, F. A thermoresponsive hydrophobically modified hydroxypropylmethylcellulose/cyclodextrin injectable hydrogel for the sustained release of drugs. *Int. J. Pharm.* **2020**, *575*, 118845. [[CrossRef](#)]
51. Lee, S.Y.; Jeon, S.I.; Sim, S.B.; Byun, Y.; Ahn, C.-H. A supramolecular host-guest interaction-mediated injectable hydrogel system with enhanced stability and sustained protein release. *Acta Biomater.* **2021**, *131*, 286–301. [[CrossRef](#)]
52. Lim, H.L.; Hwang, Y.; Kar, M.; Varghese, S. Smart hydrogels as functional biomimetic systems. *Biomater. Sci.* **2014**, *2*, 603–618. [[CrossRef](#)]
53. El-Sayed, N.S.; Hashem, A.H.; Kamel, S. Preparation and characterization of Gum Arabic Schiff’s bases based on 9-aminoacridine with in vitro evaluation of their antimicrobial and antitumor potentiality. *Carbohydr. Polym.* **2022**, *277*, 118823. [[CrossRef](#)]
54. Mi, F.-L.; Kuan, C.-Y.; Shyu, S.-S.; Lee, S.-T.; Chang, S.-F. The study of gelation kinetics and chain-relaxation properties of glutaraldehyde-cross-linked chitosan gel and their effects on microspheres preparation and drug release. *Carbohydr. Polym.* **2000**, *41*, 389–396. [[CrossRef](#)]
55. Gupta, K.C.; Jabrail, F.H. Glutaraldehyde and glyoxal cross-linked chitosan microspheres for controlled delivery of centchroman. *Carbohydr. Res.* **2006**, *341*, 744–756. [[CrossRef](#)]
56. Feng, X.; Li, D.; Han, J.; Zhuang, X.; Ding, J. Schiff base bond-linked polysaccharide–doxorubicin conjugate for upregulated cancer therapy. *Mater. Sci. Eng. C* **2017**, *76*, 1121–1128. [[CrossRef](#)]
57. Su, H.; Zhang, W.; Wu, Y.; Han, X.; Liu, G.; Jia, Q.; Shan, S. Schiff base-containing dextran nanogel as pH-sensitive drug delivery system of doxorubicin: Synthesis and characterization. *J. Biomater. Appl.* **2018**, *33*, 170–181. [[CrossRef](#)]
58. Millan, C.; Cavalli, E.; Groth, T.; Maniura-Weber, K.; Zenobi-Wong, M. Engineered microtissues formed by schiff base crosslinking restore the chondrogenic potential of aged mesenchymal stem cells. *Adv. Healthc. Mater.* **2015**, *4*, 1348–1358. [[CrossRef](#)]
59. Thomas, J.; Sharma, A.; Panwar, V.; Chopra, V.; Ghosh, D. Polysaccharide-based hybrid self-healing hydrogel supports the paracrine response of mesenchymal stem cells. *ACS Appl. Bio Mater.* **2019**, *2*, 2013–2027. [[CrossRef](#)]
60. Liu, J.; Li, J.; Yu, F.; Zhao, Y.-X.; Mo, X.-M.; Pan, J.-F. In situ forming hydrogel of natural polysaccharides through Schiff base reaction for soft tissue adhesive and hemostasis. *Int. J. Biol. Macromol.* **2020**, *147*, 653–666. [[CrossRef](#)]
61. Tan, H.; Chu, C.R.; Payne, K.A.; Marra, K.G. Injectable in situ forming biodegradable chitosan–hyaluronic acid based hydrogels for cartilage tissue engineering. *Biomaterials* **2009**, *30*, 2499–2506. [[CrossRef](#)]
62. Xu, J.; Liu, Y.; Hsu, S.-H. Hydrogels based on Schiff base linkages for biomedical applications. *Molecules* **2019**, *24*, 3005. [[CrossRef](#)]
63. Ou, Y.; Tian, M. Advances in multifunctional chitosan-based self-healing hydrogels for biomedical application. *J. Mater. Chem. B* **2021**, *9*, 7955–7971. [[CrossRef](#)] [[PubMed](#)]

64. Li, S.; Pei, M.; Wan, T.; Yang, H.; Gu, S.; Tao, Y.; Liu, X.; Zhou, Y.; Xu, W.; Xiao, P. Self-healing hyaluronic acid hydrogels based on dynamic Schiff base linkages as biomaterials. *Carbohydr. Polym.* **2020**, *250*, 116922. [[CrossRef](#)] [[PubMed](#)]
65. Xuan, H.; Wu, S.; Fei, S.; Li, B.; Yang, Y.; Yuan, H. Injectable nanofiber-polysaccharide self-healing hydrogels for wound healing. *Mater. Sci. Eng. C* **2021**, *128*, 112264. [[CrossRef](#)]
66. Wu, S.; Zhang, Z.; Xu, R.; Wei, S.; Xiong, F.; Cui, W.; Li, B.; Xue, Y.; Xuan, H.; Yuan, H. A spray-filming, tissue-adhesive, and bioactive polysaccharide self-healing hydrogel for skin regeneration. *Mater. Des.* **2022**, *217*, 110669. [[CrossRef](#)]
67. Chen, H.; Cheng, J.; Ran, L.; Yu, K.; Lu, B.; Lan, G.; Dai, F.; Lu, F. An injectable self-healing hydrogel with adhesive and antibacterial properties effectively promotes wound healing. *Carbohydr. Polym.* **2018**, *201*, 522–531. [[CrossRef](#)] [[PubMed](#)]
68. El-Sayed, N.S.; Shirazi, A.N.; El-Meligy, M.G.; El-Ziaty, A.K.; Nagieb, Z.A.; Parang, K.; Tiwari, R.K. Design, synthesis, and evaluation of chitosan conjugated GGRGDSK peptides as a cancer cell-targeting molecular transporter. *Int. J. Biol. Macromol.* **2016**, *87*, 611–622. [[CrossRef](#)]
69. Hu, H.; Li, Y.; Zhou, Q.; Ao, Y.; Yu, C.; Wan, Y.; Xu, H.; Li, Z.; Yang, X. Redox-sensitive hydroxyethyl starch–doxorubicin conjugate for tumor targeted drug delivery. *ACS Appl. Mater. Interfaces* **2016**, *8*, 30833–30844. [[CrossRef](#)]
70. Karvinen, J.; Koivisto, J.T.; Jönkkäri, I.; Kellomäki, M. The production of injectable hydrazone crosslinked gellan gum-hyaluronan-hydrogels with tunable mechanical and physical properties. *J. Mech. Behav. Biomed. Mater.* **2017**, *71*, 383–391. [[CrossRef](#)]
71. Fiorica, C.; Palumbo, F.S.; Pitarresi, G.; Puleio, R.; Condorelli, L.; Collura, G.; Giammona, G. A hyaluronic acid/cyclodextrin based injectable hydrogel for local doxorubicin delivery to solid tumors. *Int. J. Pharm.* **2020**, *589*, 119879. [[CrossRef](#)]
72. Heath, L.; Thielemans, W. Cellulose nanowhisker aerogels. *Green Chem.* **2010**, *12*, 1448–1453. [[CrossRef](#)]
73. Li, F.; Ba, Q.; Niu, S.; Guo, Y.; Duan, Y.; Zhao, P.; Lin, C.; Sun, J. In-situ forming biodegradable glycol chitosan-based hydrogels: Synthesis, characterization, and chondrocyte culture. *Mater. Sci. Eng. C* **2012**, *32*, 2017–2025. [[CrossRef](#)]
74. Liu, X.; Chen, Y.; Huang, Q.; He, W.; Feng, Q.; Yu, B. A novel thermo-sensitive hydrogel based on thiolated chitosan/hydroxyapatite/beta-glycerophosphate. *Carbohydr. Polym.* **2014**, *110*, 62–69. [[CrossRef](#)] [[PubMed](#)]
75. Summonte, S.; Racaniello, G.F.; Lopodota, A.; Denora, N.; Bernkop-Schnürch, A. Thiolated polymeric hydrogels for biomedical application: Cross-linking mechanisms. *J. Control. Release* **2021**, *330*, 470–482. [[CrossRef](#)]
76. Wu, S.-W.; Liu, X.; Miller, A.L., II; Cheng, Y.-S.; Yeh, M.-L.; Lu, L. Strengthening injectable thermo-sensitive NIPAAm-g-chitosan hydrogels using chemical cross-linking of disulfide bonds as scaffolds for tissue engineering. *Carbohydr. Polym.* **2018**, *192*, 308–316. [[CrossRef](#)] [[PubMed](#)]
77. Deng, S.; Li, X.; Yang, W.; He, K.; Ye, X. Injectable in situ cross-linking hyaluronic acid/carboxymethyl cellulose based hydrogels for drug release. *J. Biomater. Sci. Polym. Ed.* **2018**, *29*, 1643–1655. [[CrossRef](#)]
78. Lallana, E.; Fernandez-Trillo, F.; Sousa-Herves, A.; Riguera, R.; Fernandez-Megia, E. Click chemistry with polymers, dendrimers, and hydrogels for drug delivery. *Pharm. Res.* **2012**, *29*, 902–921. [[CrossRef](#)]
79. Anseth, K.S.; Klok, H.-A. Click chemistry in biomaterials, nanomedicine, and drug delivery. *Biomacromolecules* **2016**, *17*, 1–3. [[CrossRef](#)] [[PubMed](#)]
80. Takayama, Y.; Kusamori, K.; Nishikawa, M. Click chemistry as a tool for cell engineering and drug delivery. *Molecules* **2019**, *24*, 172. [[CrossRef](#)]
81. Yoon, H.Y.; Lee, D.; Lim, D.K.; Koo, H.; Kim, K. Copper-Free Click Chemistry: Applications in Drug Delivery, Cell Tracking, and Tissue Engineering. *Adv. Mater.* **2022**, *34*, 2107192. [[CrossRef](#)]
82. Zhang, J.; Xu, X.-D.; Wu, D.-Q.; Zhang, X.-Z.; Zhuo, R.-X. Synthesis of thermosensitive P (NIPAAm-co-HEMA)/cellulose hydrogels via “click” chemistry. *Carbohydr. Polym.* **2009**, *77*, 583–589. [[CrossRef](#)]
83. Li, D.-Q.; Wang, S.-Y.; Meng, Y.-J.; Guo, Z.-W.; Cheng, M.-M.; Li, J. Fabrication of self-healing pectin/chitosan hybrid hydrogel via Diels-Alder reactions for drug delivery with high swelling property, pH-responsiveness, and cytocompatibility. *Carbohydr. Polym.* **2021**, *268*, 118244. [[CrossRef](#)] [[PubMed](#)]
84. Park, S.H.; Park, J.Y.; Ji, Y.B.; Ju, H.J.; Min, B.H.; Kim, M.S. An injectable click-crosslinked hyaluronic acid hydrogel modified with a BMP-2 mimetic peptide as a bone tissue engineering scaffold. *Acta Biomater.* **2020**, *117*, 108–120. [[CrossRef](#)]
85. Wang, Q.; Xu, W.; Koppolu, R.; van Bochove, B.; Seppälä, J.; Hupa, L.; Willför, S.; Xu, C.; Wang, X. Injectable thiol-ene hydrogel of galactoglucomannan and cellulose nanocrystals in delivery of therapeutic inorganic ions with embedded bioactive glass nanoparticles. *Carbohydr. Polym.* **2022**, *276*, 118780. [[CrossRef](#)]
86. Lee, S.H.; Lee, Y.; Lee, S.W.; Ji, H.Y.; Lee, J.H.; Lee, D.S.; Park, T.G. Enzyme-mediated cross-linking of Pluronic copolymer micelles for injectable and in situ forming hydrogels. *Acta Biomater.* **2011**, *7*, 1468–1476. [[CrossRef](#)] [[PubMed](#)]
87. Teixeira, L.S.M.; Feijen, J.; van Blitterswijk, C.A.; Dijkstra, P.J.; Karperien, M. Enzyme-catalyzed crosslinkable hydrogels: Emerging strategies for tissue engineering. *Biomaterials* **2012**, *33*, 1281–1290. [[CrossRef](#)]
88. Li, J.; Zhang, D.; Guo, S.; Zhao, C.; Wang, L.; Ma, S.; Guan, F.; Yao, M. Dual-enzymatically cross-linked gelatin hydrogel promotes neural differentiation and neurotrophin secretion of bone marrow-derived mesenchymal stem cells for treatment of moderate traumatic brain injury. *Int. J. Biol. Macromol.* **2021**, *187*, 200–213. [[CrossRef](#)] [[PubMed](#)]
89. Saghati, S.; Khoshfetrat, A.B.; Tayefi Nasrabadi, H.; Roshangar, L.; Rahbarghazi, R. Fabrication of alginate-based hydrogel cross-linked via horseradish peroxidase for articular cartilage engineering. *BMC Res. Notes* **2021**, *14*, 384. [[CrossRef](#)] [[PubMed](#)]
90. Zhong, Y.; Wang, J.; Yuan, Z.; Wang, Y.; Xi, Z.; Li, L.; Liu, Z.; Guo, X. A mussel-inspired carboxymethyl cellulose hydrogel with enhanced adhesiveness through enzymatic crosslinking. *Colloids Surf. B Biointerfaces* **2019**, *179*, 462–469. [[CrossRef](#)] [[PubMed](#)]

91. Zhang, Y.; Chen, H.; Zhang, T.; Zan, Y.; Ni, T.; Cao, Y.; Wang, J.; Liu, M.; Pei, R. Injectable hydrogels from enzyme-catalyzed crosslinking as BMSCs-laden scaffold for bone repair and regeneration. *Mater. Sci. Eng. C* **2019**, *96*, 841–849. [[CrossRef](#)]
92. Wang, L.; Li, J.; Zhang, D.; Ma, S.; Zhang, J.; Gao, F.; Guan, F.; Yao, M. Dual-enzymatically crosslinked and injectable hyaluronic acid hydrogels for potential application in tissue engineering. *RSC Adv.* **2020**, *10*, 2870–2876. [[CrossRef](#)] [[PubMed](#)]
93. Nezhad-Mokhtari, P.; Ghorbani, M.; Roshangar, L.; Rad, J.S. Chemical gelling of hydrogels-based biological macromolecules for tissue engineering: Photo-and enzymatic-crosslinking methods. *Int. J. Biol. Macromol.* **2019**, *139*, 760–772. [[CrossRef](#)]
94. Chu, W.; Nie, M.; Ke, X.; Luo, J.; Li, J. Recent advances in injectable dual crosslinking hydrogels for biomedical applications. *Macromol. Biosci.* **2021**, *21*, 2100109. [[CrossRef](#)]
95. Lim, K.S.; Klotz, B.J.; Lindberg, G.C.; Melchels, F.P.; Hooper, G.J.; Malda, J.; Gawlitta, D.; Woodfield, T.B. Visible light cross-linking of gelatin hydrogels offers an enhanced cell microenvironment with improved light penetration depth. *Macromol. Biosci.* **2019**, *19*, 1900098. [[CrossRef](#)]
96. Wei, H.; Zhang, B.; Lei, M.; Lu, Z.; Liu, J.; Guo, B.; Yu, Y. Visible-Light-Mediated Nano-biom mineralization of Customizable Tough Hydrogels for Biomimetic Tissue Engineering. *ACS Nano* **2022**, *16*, 4734–4745. [[CrossRef](#)]
97. Zhao, H.; Zhang, Y.; Liu, Y.; Zheng, P.; Gao, T.; Cao, Y.; Liu, X.; Yin, J.; Pei, R. In Situ Forming Cellulose Nanofibril-Reinforced Hyaluronic Acid Hydrogel for Cartilage Regeneration. *Biomacromolecules* **2021**, *22*, 5097–5107. [[CrossRef](#)]
98. Wang, L.; Zhang, X.; Yang, K.; Fu, Y.V.; Xu, T.; Li, S.; Zhang, D.; Wang, L.N.; Lee, C.S. A novel double-crosslinking-double-network design for injectable hydrogels with enhanced tissue adhesion and antibacterial capability for wound treatment. *Adv. Funct. Mater.* **2020**, *30*, 1904156. [[CrossRef](#)]
99. Jain, K.K. Current status and future prospects of drug delivery systems. *Drug Deliv. Syst.* **2014**, *1141*, 1–56.
100. Jain, K.K. An overview of drug delivery systems. *Drug Deliv. Syst.* **2020**, *2059*, 1–54.
101. Lim, S.; Park, J.; Shim, M.K.; Um, W.; Yoon, H.Y.; Ryu, J.H.; Lim, D.K.; Kim, K. Recent advances and challenges of repurposing nanoparticle-based drug delivery systems to enhance cancer immunotherapy. *Theranostics* **2019**, *9*, 7906. [[CrossRef](#)]
102. Park, S.E.; El-Sayed, N.S.; Shamloo, K.; Lohan, S.; Kumar, S.; Sajid, M.I.; Tiwari, R.K. Targeted Delivery of Cabazitaxel Using Cyclic Cell-Penetrating Peptide and Biomarkers of Extracellular Matrix for Prostate and Breast Cancer Therapy. *Bioconjugate Chem.* **2021**, *32*, 1898–1914. [[CrossRef](#)] [[PubMed](#)]
103. Sajid, M.I.; Mandal, D.; El-Sayed, N.S.; Lohan, S.; Moreno, J.; Tiwari, R.K. Oleyl Conjugated Histidine-Arginine Cell-Penetrating Peptides as Promising Agents for siRNA Delivery. *Pharmaceutics* **2022**, *14*, 881. [[CrossRef](#)] [[PubMed](#)]
104. Nasrolahi Shirazi, A.; Salem El-Sayed, N.; Kumar Tiwari, R.; Tavakoli, K.; Parang, K. Cyclic peptide containing hydrophobic and positively charged residues as a drug delivery system for curcumin. *Curr. Drug Deliv.* **2016**, *13*, 409–417. [[CrossRef](#)]
105. El-Sayed, N.S.; Shirazi, A.N.; Sajid, M.I.; Park, S.E.; Parang, K.; Tiwari, R.K. Synthesis and antiproliferative activities of conjugates of paclitaxel and camptothecin with a cyclic cell-penetrating peptide. *Molecules* **2019**, *24*, 1427. [[CrossRef](#)] [[PubMed](#)]
106. Cirillo, G.; Spizzirri, U.G.; Curcio, M.; Nicoletta, F.P.; Iemma, F. Injectable hydrogels for cancer therapy over the last decade. *Pharmaceutics* **2019**, *11*, 486. [[CrossRef](#)] [[PubMed](#)]
107. Zhang, Y.; Tao, L.; Li, S.; Wei, Y. Synthesis of multiresponsive and dynamic chitosan-based hydrogels for controlled release of bioactive molecules. *Biomacromolecules* **2011**, *12*, 2894–2901. [[CrossRef](#)]
108. Yan, X.; Wang, F.; Zheng, B.; Huang, F. Stimuli-responsive supramolecular polymeric materials. *Chem. Soc. Rev.* **2012**, *41*, 6042–6065. [[CrossRef](#)]
109. Kocak, G.; Tuncer, C.; Bütün, V. pH-Responsive polymers. *Polym. Chem.* **2017**, *8*, 144–176. [[CrossRef](#)]
110. Choi, B.; Kim, S.; Lin, B.; Li, K.; Bezougliaia, O.; Kim, J.; Evseenko, D.; Aghaloo, T.; Lee, M. Visible-light-initiated hydrogels preserving cartilage extracellular signaling for inducing chondrogenesis of mesenchymal stem cells. *Acta Biomater.* **2015**, *12*, 30–41. [[CrossRef](#)]
111. Gao, Y.; Wei, Z.; Li, F.; Yang, Z.M.; Chen, Y.M.; Zrinyi, M.; Osada, Y. Synthesis of a morphology controllable Fe₃O₄ nanoparticle/hydrogel magnetic nanocomposite inspired by magnetotactic bacteria and its application in H₂O₂ detection. *Green Chem.* **2014**, *16*, 1255–1261. [[CrossRef](#)]
112. Zhang, Z.P.; Rong, M.Z.; Zhang, M.Q. Polymer engineering based on reversible covalent chemistry: A promising innovative pathway towards new materials and new functionalities. *Prog. Polym. Sci.* **2018**, *80*, 39–93. [[CrossRef](#)]
113. Qu, J.; Zhao, X.; Ma, P.X.; Guo, B. pH-responsive self-healing injectable hydrogel based on N-carboxyethyl chitosan for hepatocellular carcinoma therapy. *Acta Biomater.* **2017**, *58*, 168–180. [[CrossRef](#)] [[PubMed](#)]
114. Chen, N.; Wang, H.; Ling, C.; Vermerris, W.; Wang, B.; Tong, Z. Cellulose-based injectable hydrogel composite for pH-responsive and controllable drug delivery. *Carbohydr. Polym.* **2019**, *225*, 115207. [[CrossRef](#)] [[PubMed](#)]
115. Khan, S.; Minhas, M.U.; Ahmad, M.; Sohail, M. Self-assembled supramolecular thermoreversible β -cyclodextrin/ethylene glycol injectable hydrogels with difunctional Pluronic® 127 as controlled delivery depot of curcumin. Development, characterization and in vitro evaluation. *J. Biomater. Sci. Polym. Ed.* **2018**, *29*, 1–34. [[CrossRef](#)] [[PubMed](#)]
116. Chen, B.; Liang, Y.; Zhang, J.; Bai, L.; Xu, M.; Han, Q.; Han, X.; Xiu, J.; Li, M.; Zhou, X. Synergistic enhancement of tendon-to-bone healing via anti-inflammatory and pro-differentiation effects caused by sustained release of Mg²⁺/curcumin from injectable self-healing hydrogels. *Theranostics* **2021**, *11*, 5911. [[CrossRef](#)] [[PubMed](#)]
117. Yuan, L.; Li, Z.; Li, X.; Qiu, S.; Lei, J.; Li, D.; Mu, C.; Ge, L. Functionalization of an Injectable Self-Healing pH-Responsive Hydrogel by Incorporating a Curcumin/Polymerized β -Cyclodextrin Inclusion Complex for Selective Toxicity to Osteosarcoma. *ACS Appl. Polym. Mater.* **2022**, *4*, 1243–1254. [[CrossRef](#)]

118. Ning, P.; Lü, S.; Bai, X.; Wu, X.; Gao, C.; Wen, N.; Liu, M. High encapsulation and localized delivery of curcumin from an injectable hydrogel. *Mater. Sci. Eng. C* **2018**, *83*, 121–129. [[CrossRef](#)]
119. Hoque, J.; Bhattacharjee, B.; Prakash, R.G.; Paramanandham, K.; Haldar, J. Dual function injectable hydrogel for controlled release of antibiotic and local antibacterial therapy. *Biomacromolecules* **2018**, *19*, 267–278. [[CrossRef](#)]
120. Vulic, K.; Shoichet, M.S. Tunable growth factor delivery from injectable hydrogels for tissue engineering. *J. Am. Chem. Soc.* **2012**, *134*, 882–885. [[CrossRef](#)]
121. Li, H.; Koenig, A.M.; Sloan, P.; Leipzig, N.D. In vivo assessment of guided neural stem cell differentiation in growth factor immobilized chitosan-based hydrogel scaffolds. *Biomaterials* **2014**, *35*, 9049–9057. [[CrossRef](#)]
122. Schneider, M.C.; Chu, S.; Randolph, M.A.; Bryant, S.J. An in vitro and in vivo comparison of cartilage growth in chondrocyte-laden matrix metalloproteinase-sensitive poly (ethylene glycol) hydrogels with localized transforming growth factor β 3. *Acta Biomater.* **2019**, *93*, 97–110. [[CrossRef](#)] [[PubMed](#)]
123. Ma, X.; Xu, T.; Chen, W.; Qin, H.; Chi, B.; Ye, Z. Injectable hydrogels based on the hyaluronic acid and poly (γ -glutamic acid) for controlled protein delivery. *Carbohydr. Polym.* **2018**, *179*, 100–109. [[CrossRef](#)]
124. Xu, Y.; Lu, G.; Chen, M.; Wang, P.; Li, Z.; Han, X.; Liang, J.; Sun, Y.; Fan, Y.; Zhang, X. Redox and pH dual-responsive injectable hyaluronan hydrogels with shape-recovery and self-healing properties for protein and cell delivery. *Carbohydr. Polym.* **2020**, *250*, 116979. [[CrossRef](#)] [[PubMed](#)]
125. Henry, N.; Clouet, J.; Fragale, A.; Griveau, L.; Chédeville, C.; Véziers, J.; Weiss, P.; Le Bideau, J.; Guicheux, J.; Le Visage, C. Pullulan microbeads/Si-HPMC hydrogel injectable system for the sustained delivery of GDF-5 and TGF- β 1: New insight into intervertebral disc regenerative medicine. *Drug Deliv.* **2017**, *24*, 999–1010. [[CrossRef](#)] [[PubMed](#)]
126. Gu, Z.; Aimetti, A.A.; Wang, Q.; Dang, T.T.; Zhang, Y.; Veisoh, O.; Cheng, H.; Langer, R.S.; Anderson, D.G. Injectable nano-network for glucose-mediated insulin delivery. *ACS Nano* **2013**, *7*, 4194–4201. [[CrossRef](#)]
127. Divband, B.; Aghazadeh, M.; Al-Qaim, Z.H.; Samiei, M.; Hussein, F.H.; Shaabani, A.; Shahi, S.; Sedghi, R. Bioactive chitosan biguanidine-based injectable hydrogels as a novel BMP-2 and VEGF carrier for osteogenesis of dental pulp stem cells. *Carbohydr. Polym.* **2021**, *273*, 118589. [[CrossRef](#)]
128. Ballios, B.G.; Cooke, M.J.; Donaldson, L.; Coles, B.L.; Morshead, C.M.; van der Kooy, D.; Shoichet, M.S. A hyaluronan-based injectable hydrogel improves the survival and integration of stem cell progeny following transplantation. *Stem Cell Rep.* **2015**, *4*, 1031–1045. [[CrossRef](#)]
129. Sisso, A.M.; Boit, M.O.; DeForest, C.A. Self-healing injectable gelatin hydrogels for localized therapeutic cell delivery. *J. Biomed. Mater. Res. Part A* **2020**, *108*, 1112–1121. [[CrossRef](#)]
130. Bhattacharjee, M.; Escobar Ivirico, J.L.; Kan, H.-M.; Shah, S.; Otsuka, T.; Bordett, R.; Barajaa, M.; Nagiah, N.; Pandey, R.; Nair, L.S. Injectable amnion hydrogel-mediated delivery of adipose-derived stem cells for osteoarthritis treatment. *Proc. Natl. Acad. Sci. USA* **2022**, *119*, e2120968119. [[CrossRef](#)]
131. Anamizu, M.; Tabata, Y. Design of injectable hydrogels of gelatin and alginate with ferric ions for cell transplantation. *Acta Biomater.* **2019**, *100*, 184–190. [[CrossRef](#)] [[PubMed](#)]
132. Miller, B.; Hansrisuk, A.; Highley, C.B.; Caliani, S.R. Guest–host supramolecular assembly of injectable hydrogel nanofibers for cell encapsulation. *ACS Biomater. Sci. Eng.* **2021**, *7*, 4164–4174. [[CrossRef](#)] [[PubMed](#)]
133. Kim, B.-S.; Cho, C.-S. Injectable hydrogels for regenerative medicine. *Tissue Eng. Regen. Med.* **2018**, *15*, 511–512. [[CrossRef](#)]
134. Bertsch, P.; Diba, M.; Mooney, D.J.; Leeuwenburgh, S.C. Self-Healing Injectable Hydrogels for Tissue Regeneration. *Chem. Rev.* **2022**. [[CrossRef](#)]
135. Wang, B.; Liu, J.; Niu, D.; Wu, N.; Yun, W.; Wang, W.; Zhang, K.; Li, G.; Yan, S.; Xu, G. Mussel-inspired bisphosphonated injectable nanocomposite hydrogels with adhesive, self-healing, and osteogenic properties for bone regeneration. *ACS Appl. Mater. Interfaces* **2021**, *13*, 32673–32689. [[CrossRef](#)] [[PubMed](#)]
136. Gurtner, G.C.; Werner, S.; Barrandon, Y.; Longaker, M.T. Wound repair and regeneration. *Nature* **2008**, *453*, 314–321. [[CrossRef](#)]
137. Gao, Y.; Li, Z.; Huang, J.; Zhao, M.; Wu, J. In situ formation of injectable hydrogels for chronic wound healing. *J. Mater. Chem. B* **2020**, *8*, 8768–8780. [[CrossRef](#)]
138. Yan, C.; Altunbas, A.; Yucel, T.; Nagarkar, R.P.; Schneider, J.P.; Pochan, D.J. Injectable solid hydrogel: Mechanism of shear-thinning and immediate recovery of injectable β -hairpin peptide hydrogels. *Soft Matter* **2010**, *6*, 5143–5156. [[CrossRef](#)]
139. Zhao, X.; Wu, H.; Guo, B.; Dong, R.; Qiu, Y.; Ma, P.X. Antibacterial anti-oxidant electroactive injectable hydrogel as self-healing wound dressing with hemostasis and adhesiveness for cutaneous wound healing. *Biomaterials* **2017**, *122*, 34–47. [[CrossRef](#)] [[PubMed](#)]
140. Jee, J.-P.; Pangeni, R.; Jha, S.K.; Byun, Y.; Park, J.W. Preparation and in vivo evaluation of a topical hydrogel system incorporating highly skin-permeable growth factors, quercetin, and oxygen carriers for enhanced diabetic wound-healing therapy. *Int. J. Nanomed.* **2019**, *14*, 5449. [[CrossRef](#)]
141. An, Z.; Zhang, L.; Liu, Y.; Zhao, H.; Zhang, Y.; Cao, Y.; Zhang, Y.; Pei, R. Injectable thioketal-containing hydrogel dressing accelerates skin wound healing with the incorporation of reactive oxygen species scavenging and growth factor release. *Biomater. Sci.* **2022**, *10*, 100–113. [[CrossRef](#)]
142. Liu, X.; Jia, G. Modern wound dressing using polymers/biopolymers. *J. Mater. Sci. Eng.* **2018**, *7*, 3.
143. Zhu, T.; Mao, J.; Cheng, Y.; Liu, H.; Lv, L.; Ge, M.; Li, S.; Huang, J.; Chen, Z.; Li, H. Recent progress of polysaccharide-based hydrogel interfaces for wound healing and tissue engineering. *Adv. Mater. Interfaces* **2019**, *6*, 1900761. [[CrossRef](#)]

144. Shi, W.; Kong, Y.; Su, Y.; Kuss, M.A.; Jiang, X.; Li, X.; Xie, J.; Duan, B. Tannic acid-inspired, self-healing, and dual stimuli responsive dynamic hydrogel with potent antibacterial and anti-oxidative properties. *J. Mater. Chem. B* **2021**, *9*, 7182–7195. [[CrossRef](#)]
145. Wang, Y.; Garcia, C.R.; Ding, Z.; Gabriliska, R.; Rumbaugh, K.P.; Wu, J.; Liu, Q.; Li, W. Adhesive, self-healing, and antibacterial chitosan hydrogels with tunable two-layer structures. *ACS Sustain. Chem. Eng.* **2020**, *8*, 18006–18014. [[CrossRef](#)]
146. Yang, R.; Liu, X.; Ren, Y.; Xue, W.; Liu, S.; Wang, P.; Zhao, M.; Xu, H.; Chi, B. Injectable adaptive self-healing hyaluronic acid/poly (γ -glutamic acid) hydrogel for cutaneous wound healing. *Acta Biomater.* **2021**, *127*, 102–115. [[CrossRef](#)] [[PubMed](#)]
147. Zhang, K.; Yang, C.; Cheng, C.; Shi, C.; Sun, M.; Hu, H.; Shi, T.; Chen, X.; He, X.; Zheng, X. Bioactive Injectable Hydrogel Dressings for Bacteria-Infected Diabetic Wound Healing: A “Pull-Push” Approach. *ACS Appl. Mater. Interfaces* **2022**, *14*, 26404–26417. [[CrossRef](#)] [[PubMed](#)]
148. Liao, M.; Wan, P.; Wen, J.; Gong, M.; Wu, X.; Wang, Y.; Shi, R.; Zhang, L. Wearable, healable, and adhesive epidermal sensors assembled from mussel-inspired conductive hybrid hydrogel framework. *Adv. Funct. Mater.* **2017**, *27*, 1703852. [[CrossRef](#)]
149. Liu, Y.; Wang, H.; Zhao, W.; Zhang, M.; Qin, H.; Xie, Y. Flexible, stretchable sensors for wearable health monitoring: Sensing mechanisms, materials, fabrication strategies and features. *Sensors* **2018**, *18*, 645. [[CrossRef](#)]
150. Zhang, X.; Sheng, N.; Wang, L.; Tan, Y.; Liu, C.; Xia, Y.; Nie, Z.; Sui, K. Supramolecular nanofibrillar hydrogels as highly stretchable, elastic and sensitive ionic sensors. *Mater. Horiz.* **2019**, *6*, 326–333. [[CrossRef](#)]
151. Liu, Y.; He, K.; Chen, G.; Leow, W.R.; Chen, X. Nature-inspired structural materials for flexible electronic devices. *Chem. Rev.* **2017**, *117*, 12893–12941. [[CrossRef](#)]
152. Zhang, Q.; Liu, X.; Duan, L.; Gao, G. Ultra-stretchable wearable strain sensors based on skin-inspired adhesive, tough and conductive hydrogels. *Chem. Eng. J.* **2019**, *365*, 10–19. [[CrossRef](#)]
153. Liu, Y.; Zheng, H.; Liu, M. High performance strain sensors based on chitosan/carbon black composite sponges. *Mater. Des.* **2018**, *141*, 276–285. [[CrossRef](#)]
154. Kanoun, O.; Müller, C.; Benchirouf, A.; Sanli, A.; Dinh, T.N.; Al-Hamry, A.; Bu, L.; Gerlach, C.; Bouhamed, A. Flexible carbon nanotube films for high performance strain sensors. *Sensors* **2014**, *14*, 10042–10071. [[CrossRef](#)] [[PubMed](#)]
155. Liu, Q.; Chen, J.; Li, Y.; Shi, G. High-performance strain sensors with fish-scale-like graphene-sensing layers for full-range detection of human motions. *ACS Nano* **2016**, *10*, 7901–7906. [[CrossRef](#)]
156. Zhang, J.; Chen, L.; Shen, B.; Mo, J.; Tang, F.; Feng, J. Highly stretchable and self-healing double network hydrogel based on polysaccharide and polyzwitterion for wearable electric skin. *Polymer* **2020**, *194*, 122381. [[CrossRef](#)]
157. Wang, Y.; Zhang, H.; Zhang, H.; Chen, J.; Li, B.; Fu, S. Synergy coordination of cellulose-based dialdehyde and carboxyl with Fe³⁺ and recoverable conductive self-healing hydrogel for sensor. *Mater. Sci. Eng. C* **2021**, *125*, 112094. [[CrossRef](#)]
158. Pan, X.; Wang, Q.; He, P.; Liu, K.; Ni, Y.; Ouyang, X.; Chen, L.; Huang, L.; Wang, H.; Tan, Y. Mussel-inspired nanocomposite hydrogel-based electrodes with reusable and injectable properties for human electrophysiological signals detection. *ACS Sustain. Chem. Eng.* **2019**, *7*, 7918–7925. [[CrossRef](#)]
159. Fan, L.; He, Z.; Peng, X.; Xie, J.; Su, F.; Wei, D.-X.; Zheng, Y.; Yao, D. Injectable, Intrinsically Antibacterial Conductive Hydrogels with Self-Healing and pH Stimulus Responsiveness for Epidermal Sensors and Wound Healing. *ACS Appl. Mater. Interfaces* **2021**, *13*, 53541–53552. [[CrossRef](#)]
160. Zhao, M.; Zhang, W.; Sun, P.; Shi, L.; Liu, Y.; Zhang, X.; Zhang, L.; Han, W.; Chen, P. Skin-Inspired Packaging of Injectable Hydrogel Sensors Enabled by Photopolymerizable and Swellable Hydrogels toward Sustainable Electronics. *ACS Sustain. Chem. Eng.* **2022**, *20*, 6657–6666. [[CrossRef](#)]